

1

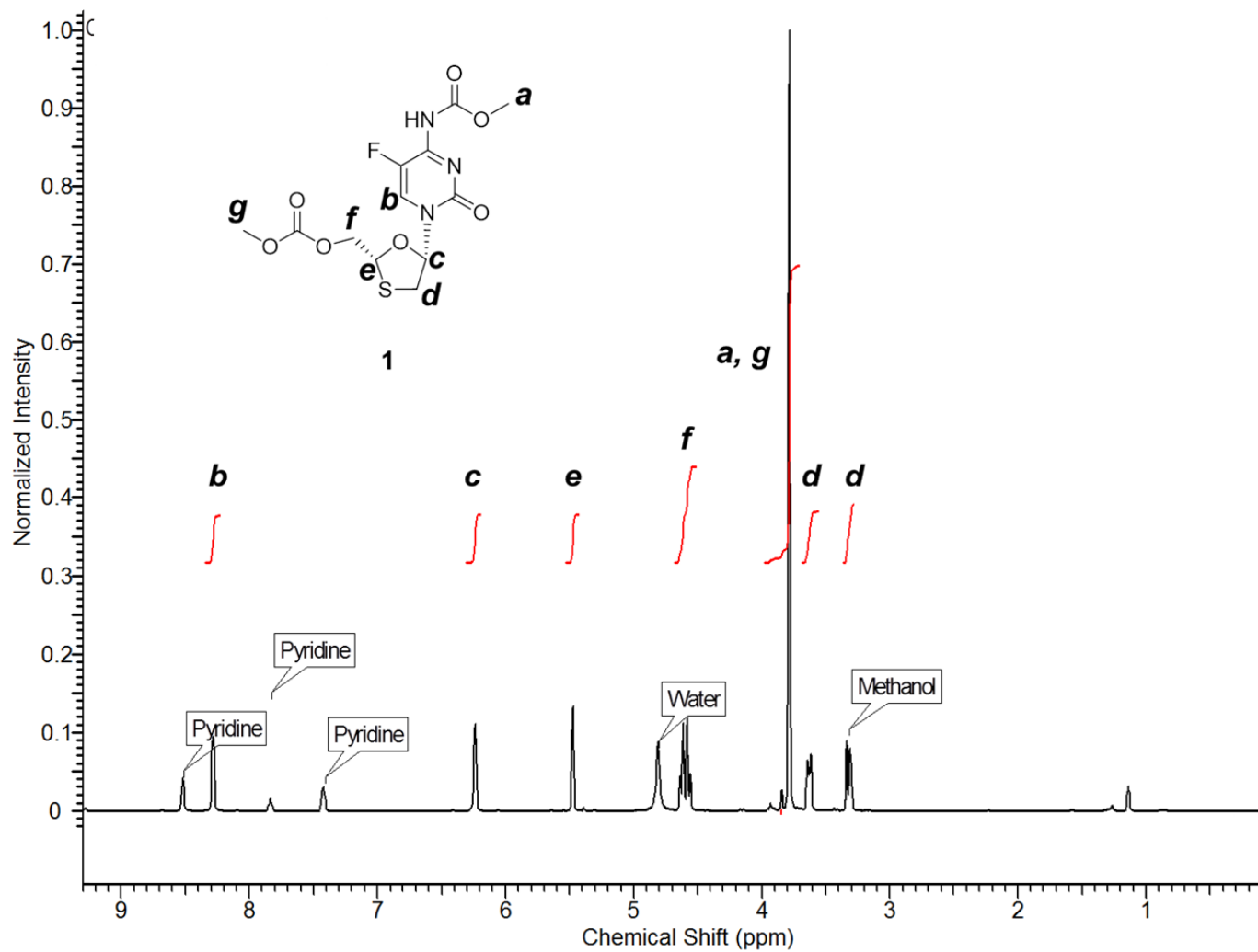
2

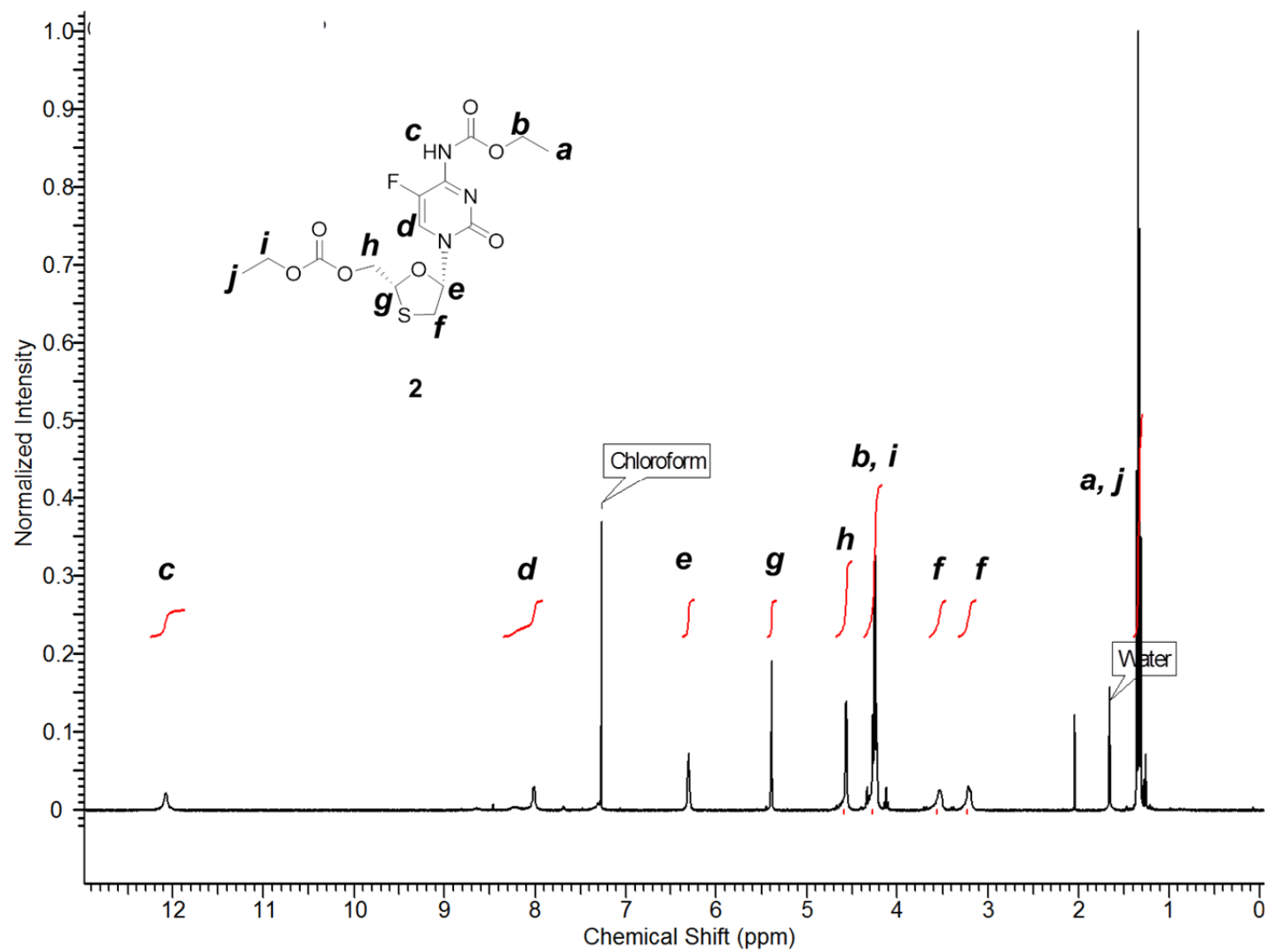
3

4 **Semi-solid prodrug nanoparticles for long-acting delivery of water-soluble**  
5 **antiretroviral drugs within combination HIV therapies**

6

7 James J. Hobson et al

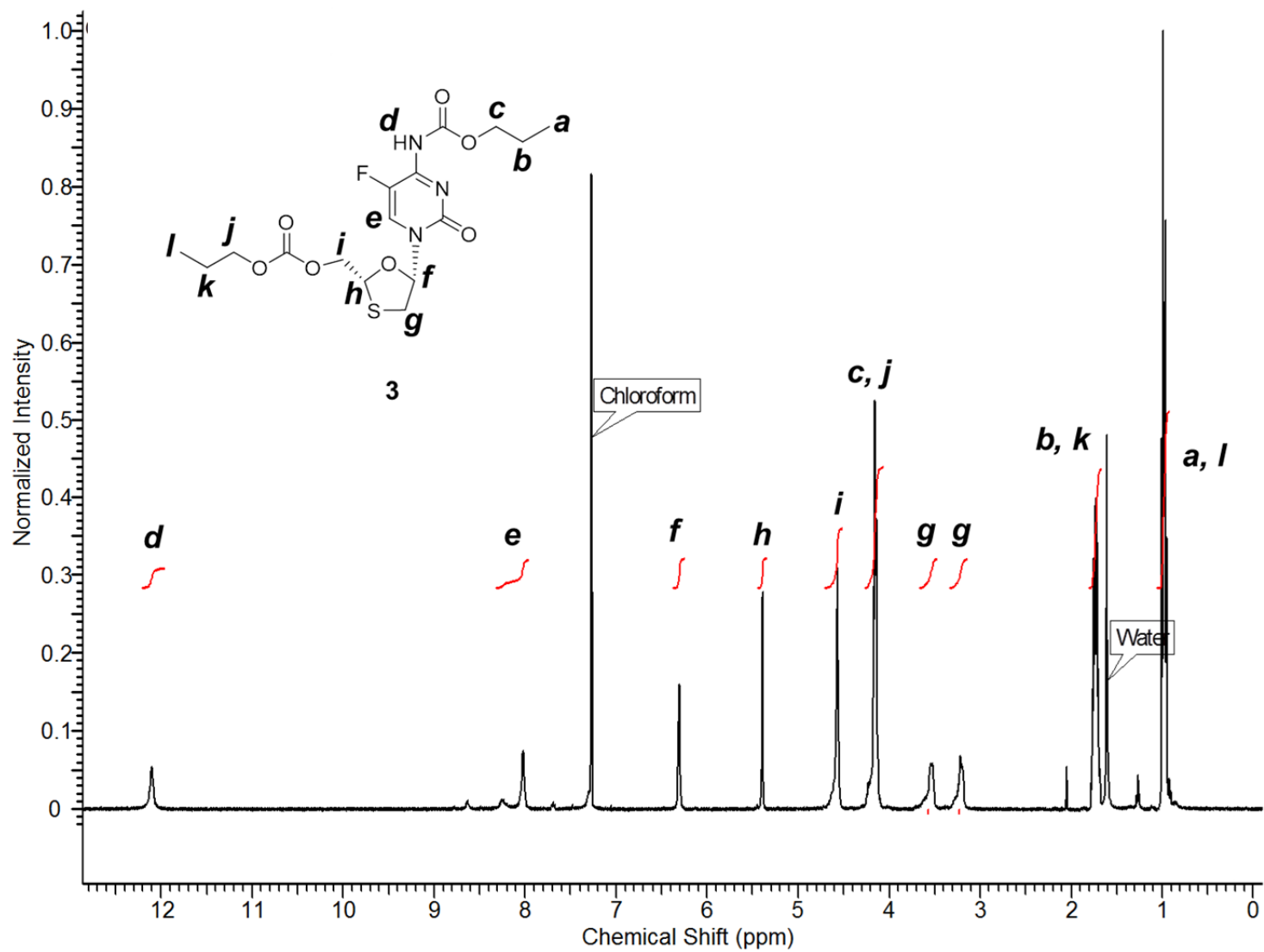




12

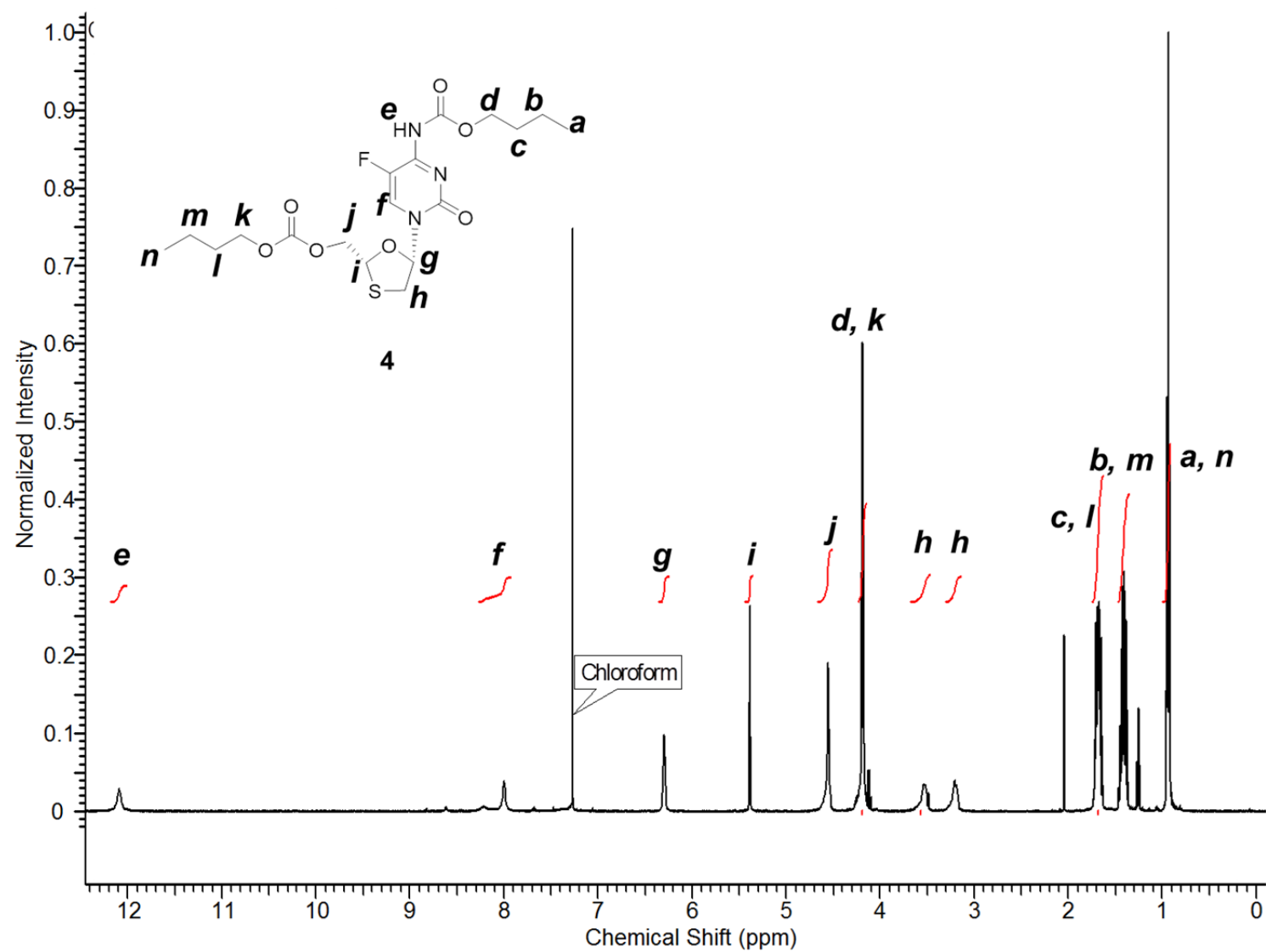
13 **Supplementary Figure 2.**  $^1\text{H}$  NMR (500 MHz) of **2** in  $\text{CDCl}_3$ .

14



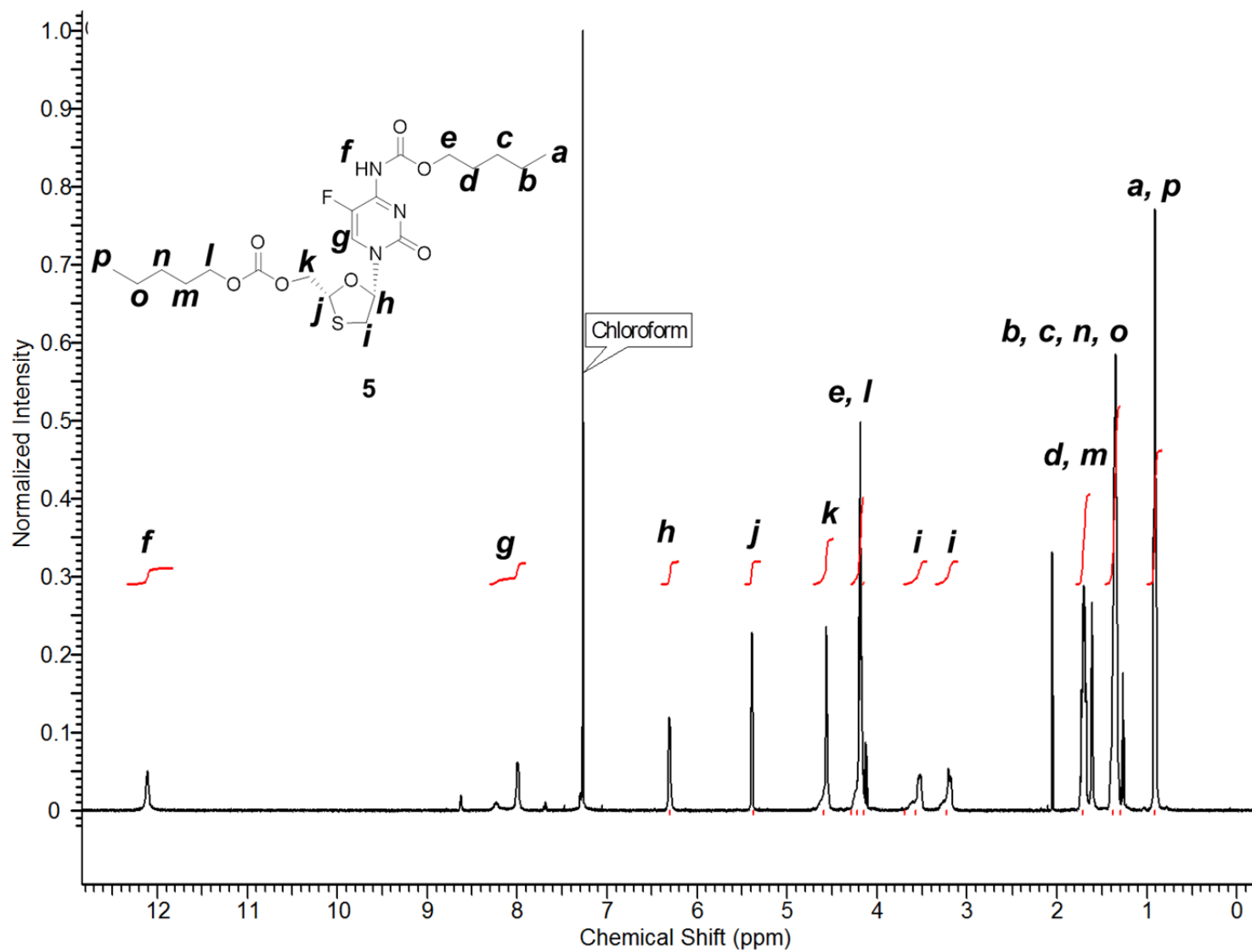
15

16 **Supplementary Figure 3.**  $^1\text{H}$  NMR (500 MHz) of **3** in  $\text{CDCl}_3$ .



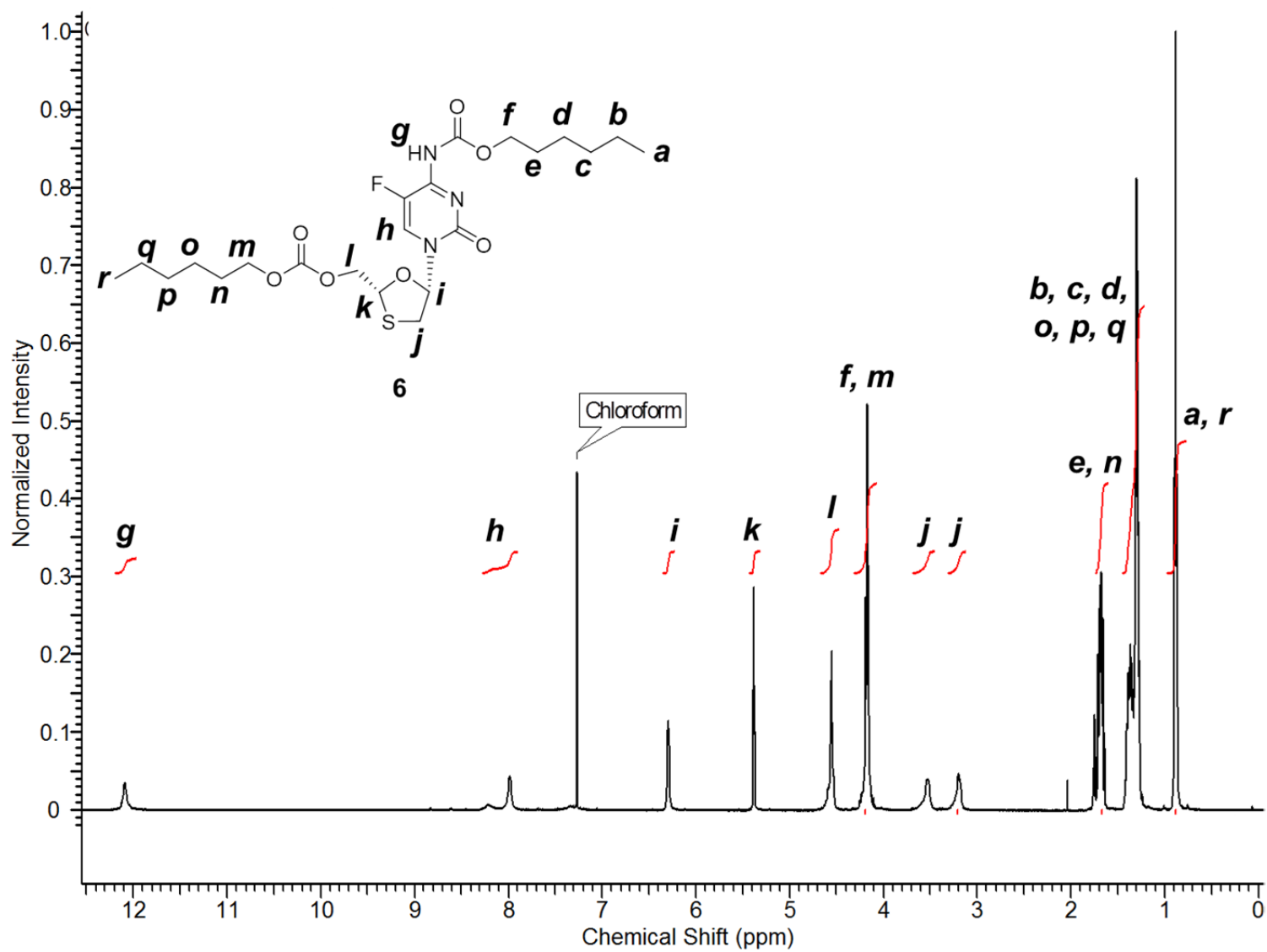
17

18 **Supplementary Figure 4.**  $^1\text{H}$  NMR (500 MHz) of **4** in  $\text{CDCl}_3$ .



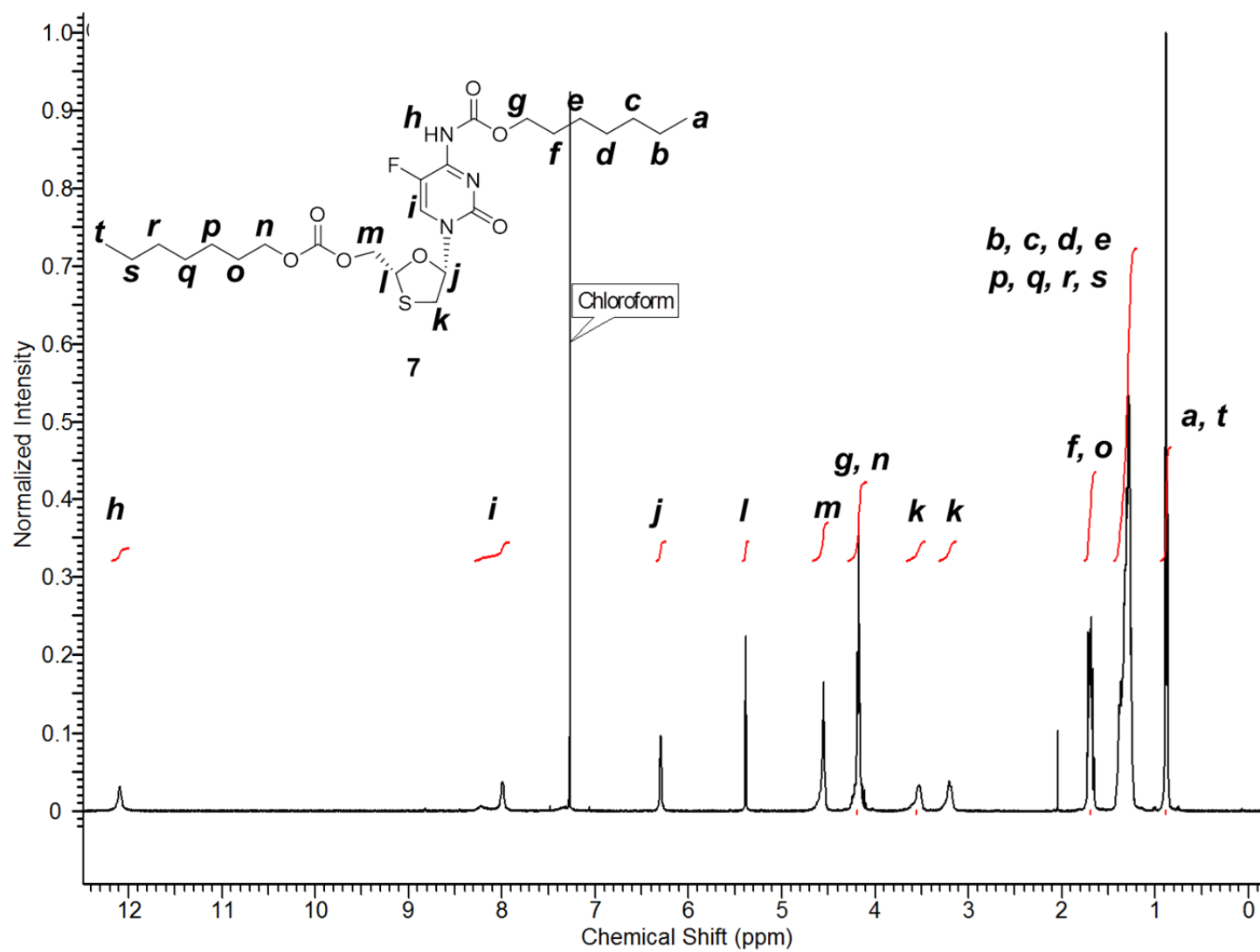
19

20 **Supplementary Figure 5.** <sup>1</sup>H NMR (500 MHz) of **5** in CDCl<sub>3</sub>.



21

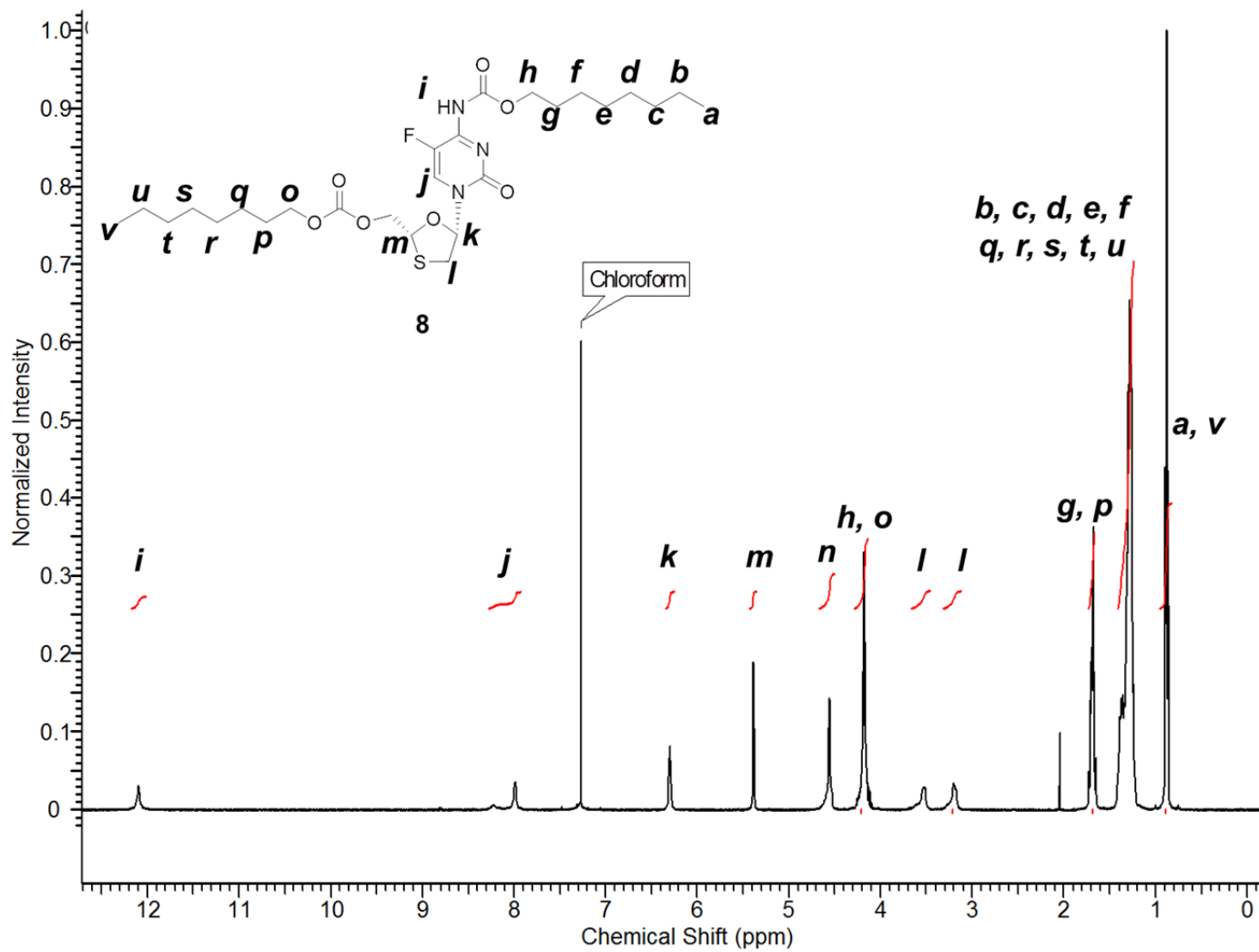
22 **Supplementary Figure 6.**  $^1\text{H}$  NMR (500 MHz) of **6** in  $\text{CDCl}_3$ .



23

24 **Supplementary Figure 7.**  $^1\text{H}$  NMR (500 MHz) of **7** in  $\text{CDCl}_3$ .

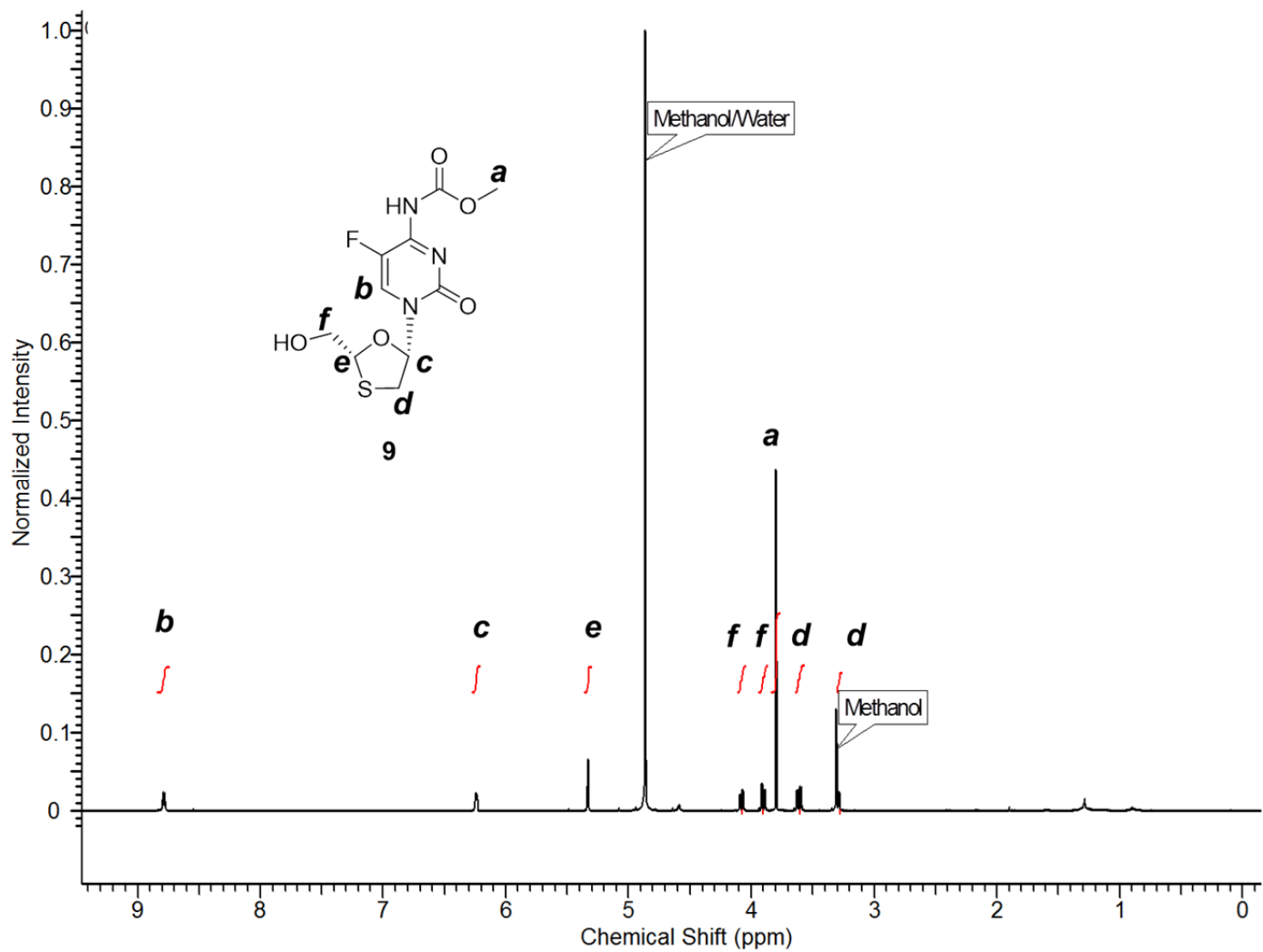




25

26 **Supplementary Figure 8.**  $^1\text{H}$  NMR (500 MHz) of **8** in  $\text{CDCl}_3$ .

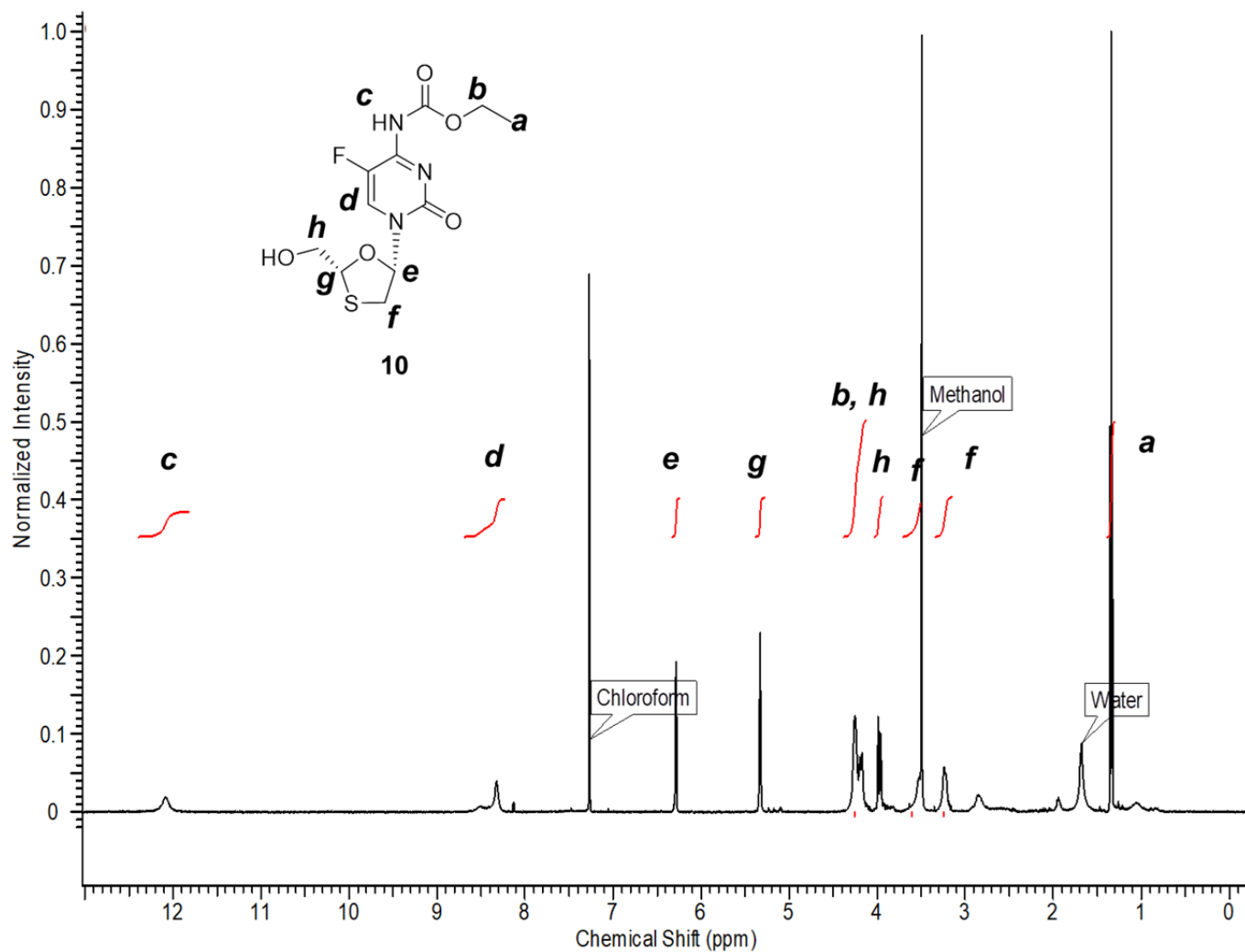
27



28

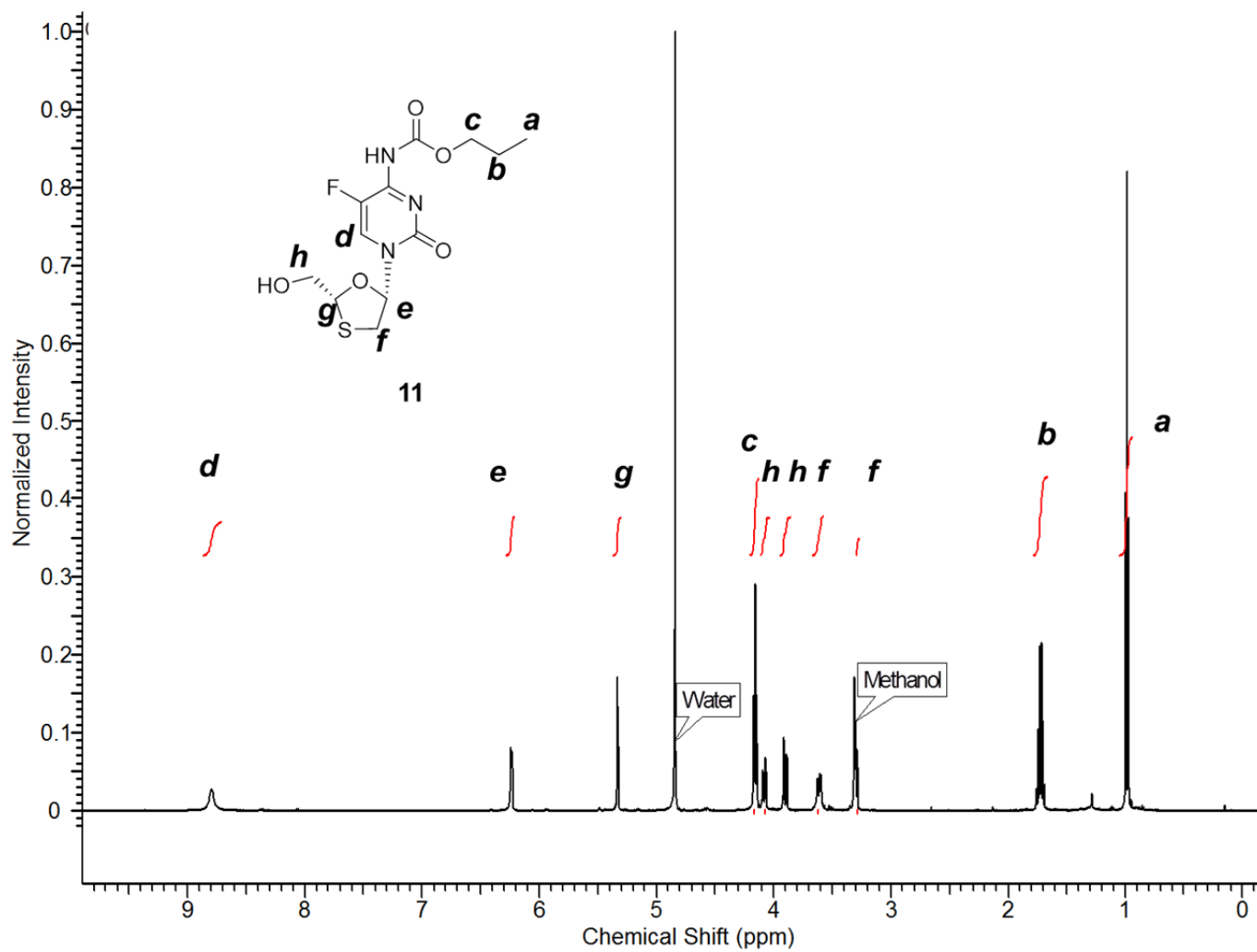
29 **Supplementary Figure 9.**  $^1\text{H}$  NMR (500 MHz) of **9** in  $\text{CD}_3\text{OD}$ .

30



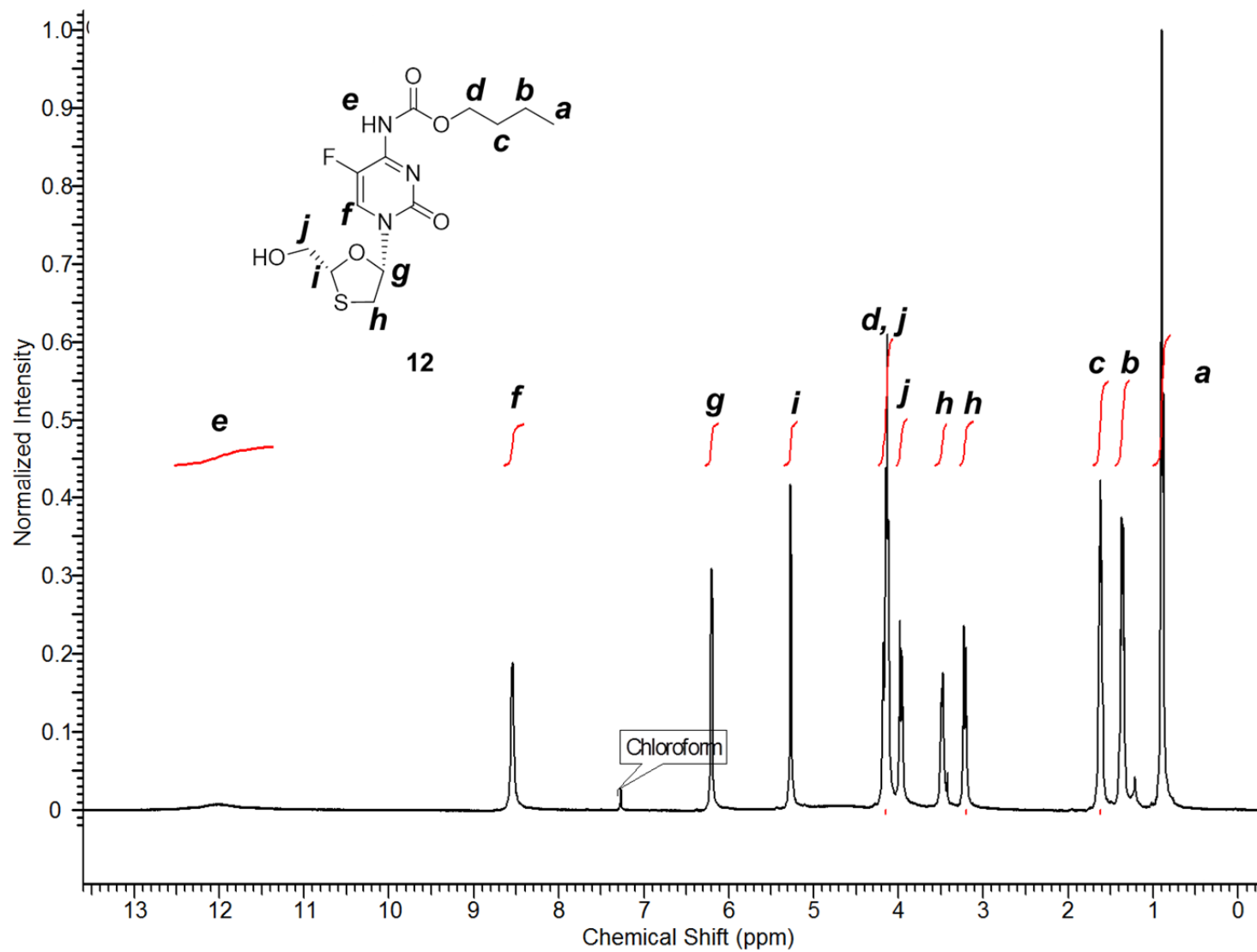
31

32 **Supplementary Figure 10.** <sup>1</sup>H NMR (500 MHz) of **10** in CDCl<sub>3</sub>.



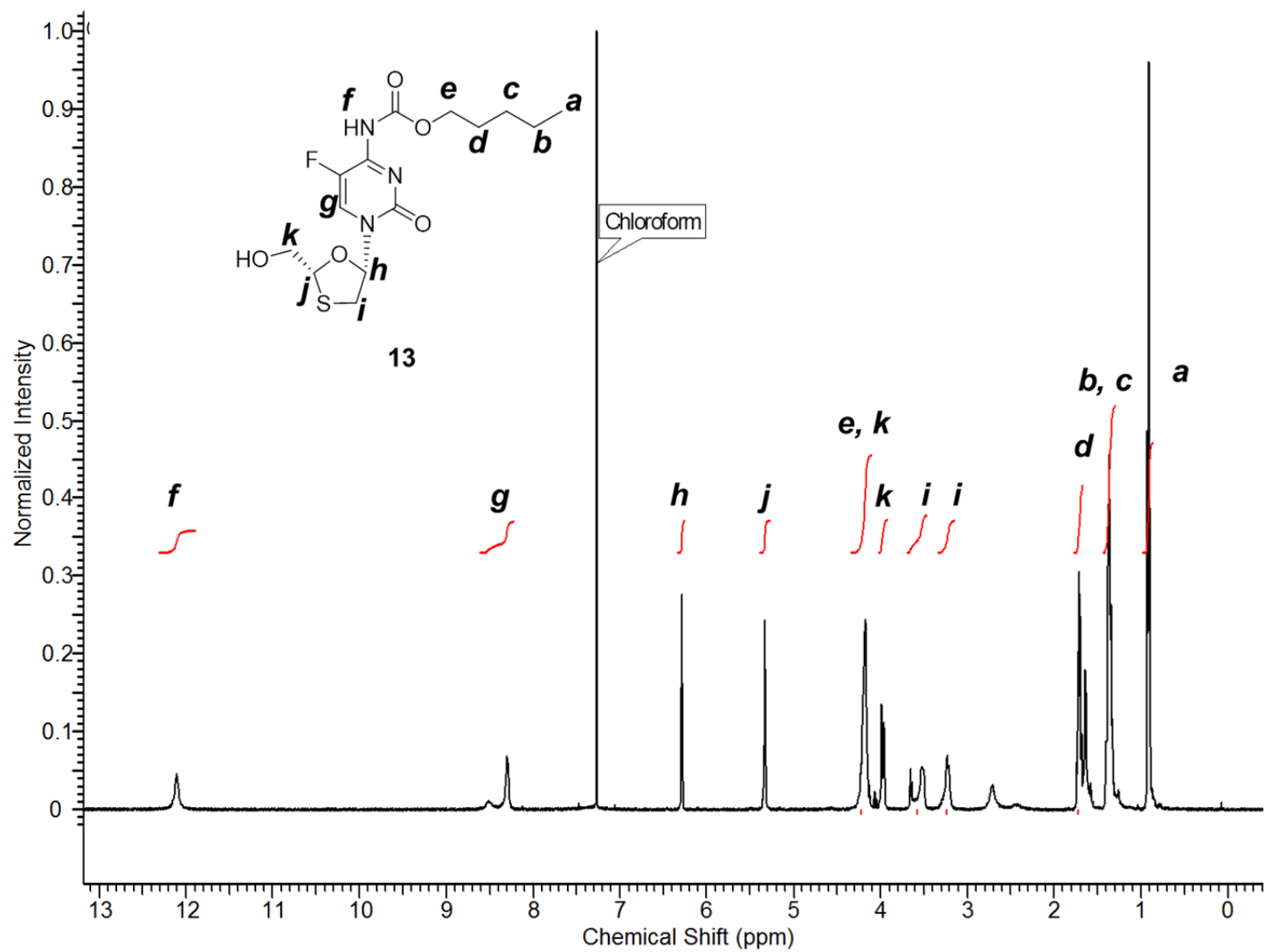
33

34 **Supplementary Figure 11.**  $^1\text{H}$  NMR (500 MHz) of **11** in  $\text{CD}_3\text{OD}$ .



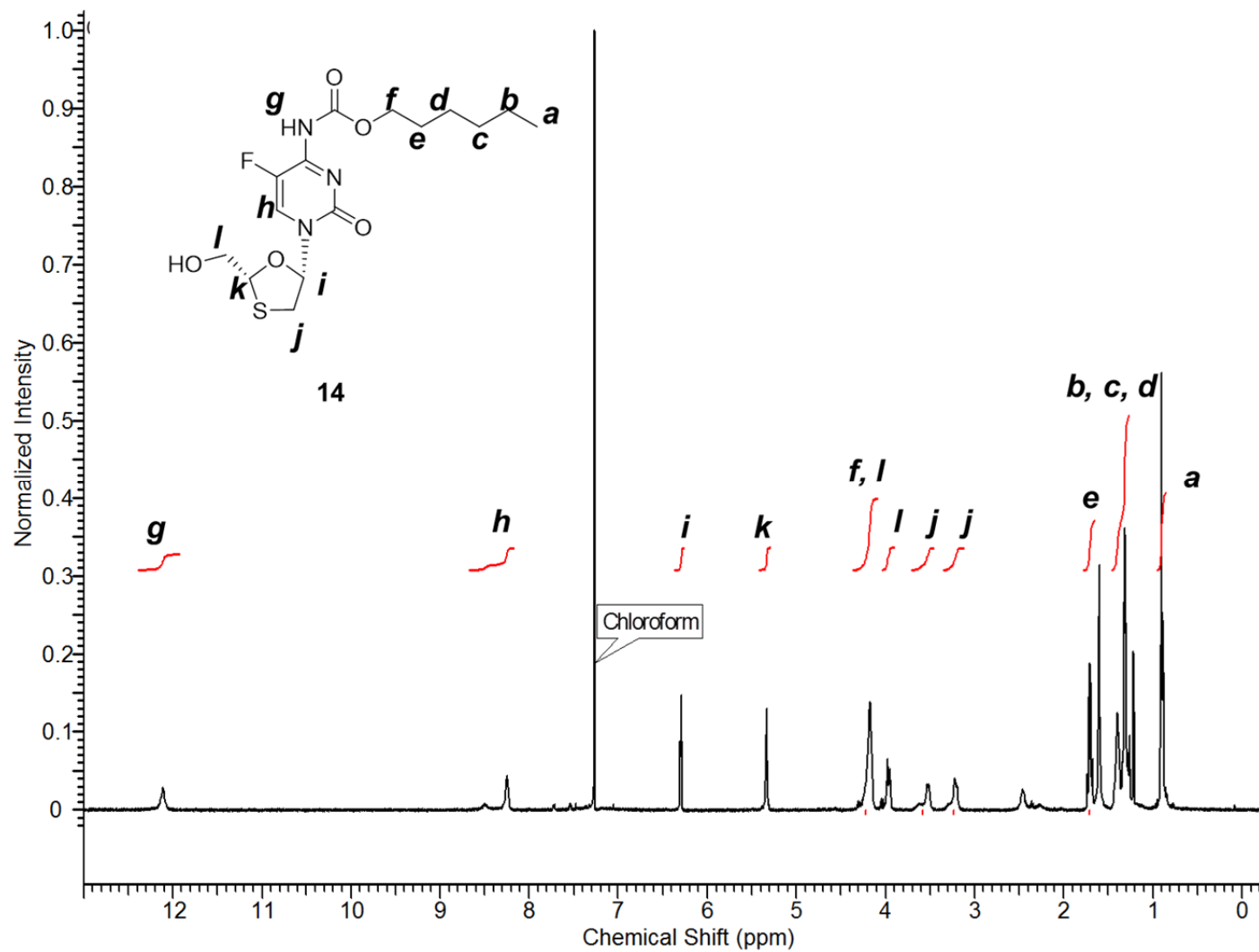
35

36 **Supplementary Figure 12.** <sup>1</sup>H NMR (500 MHz) of **12** in CDCl<sub>3</sub>.



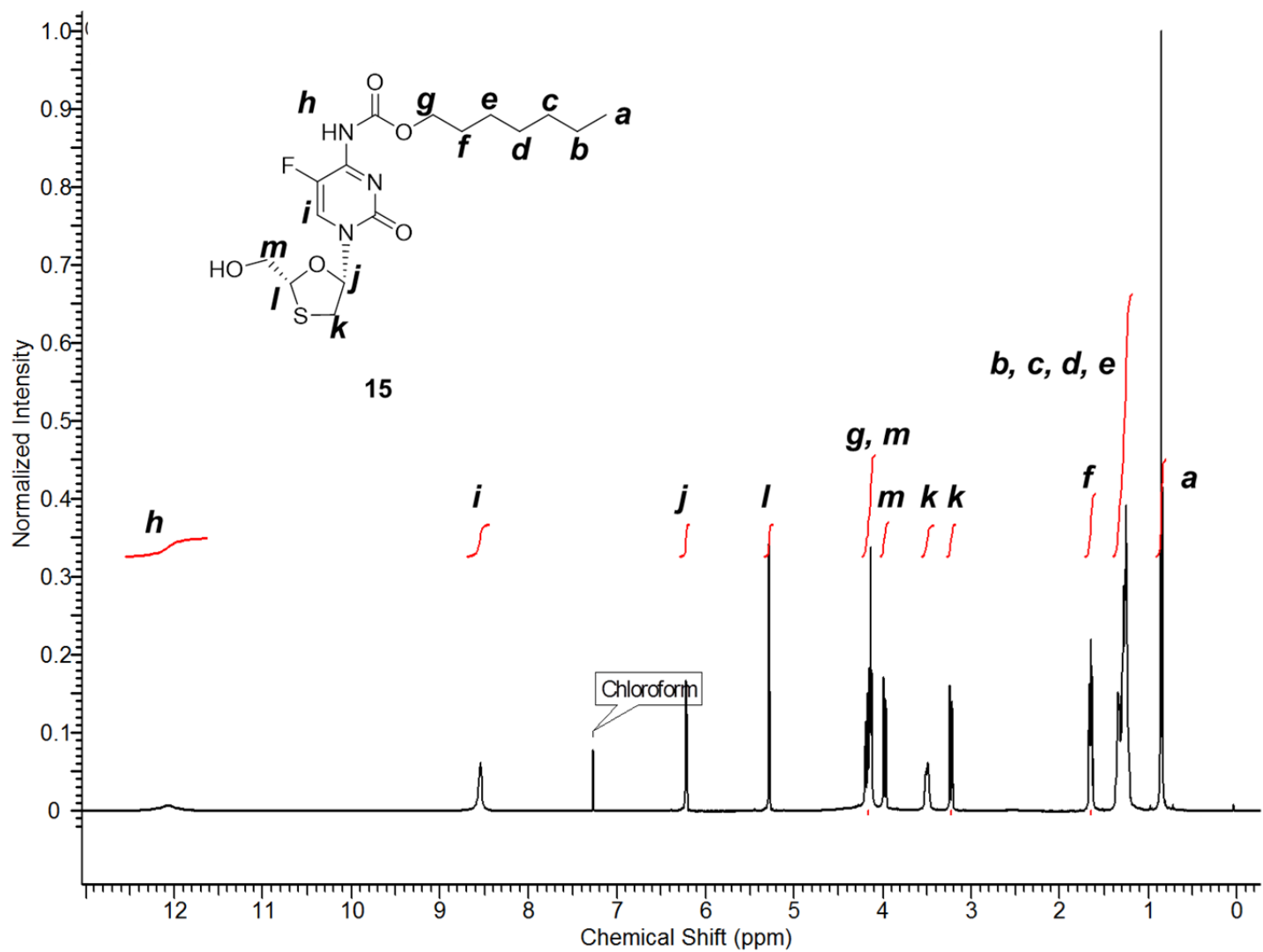
37

38 **Supplementary Figure 13.** <sup>1</sup>H NMR (500 MHz) of **13** in CDCl<sub>3</sub>.



39

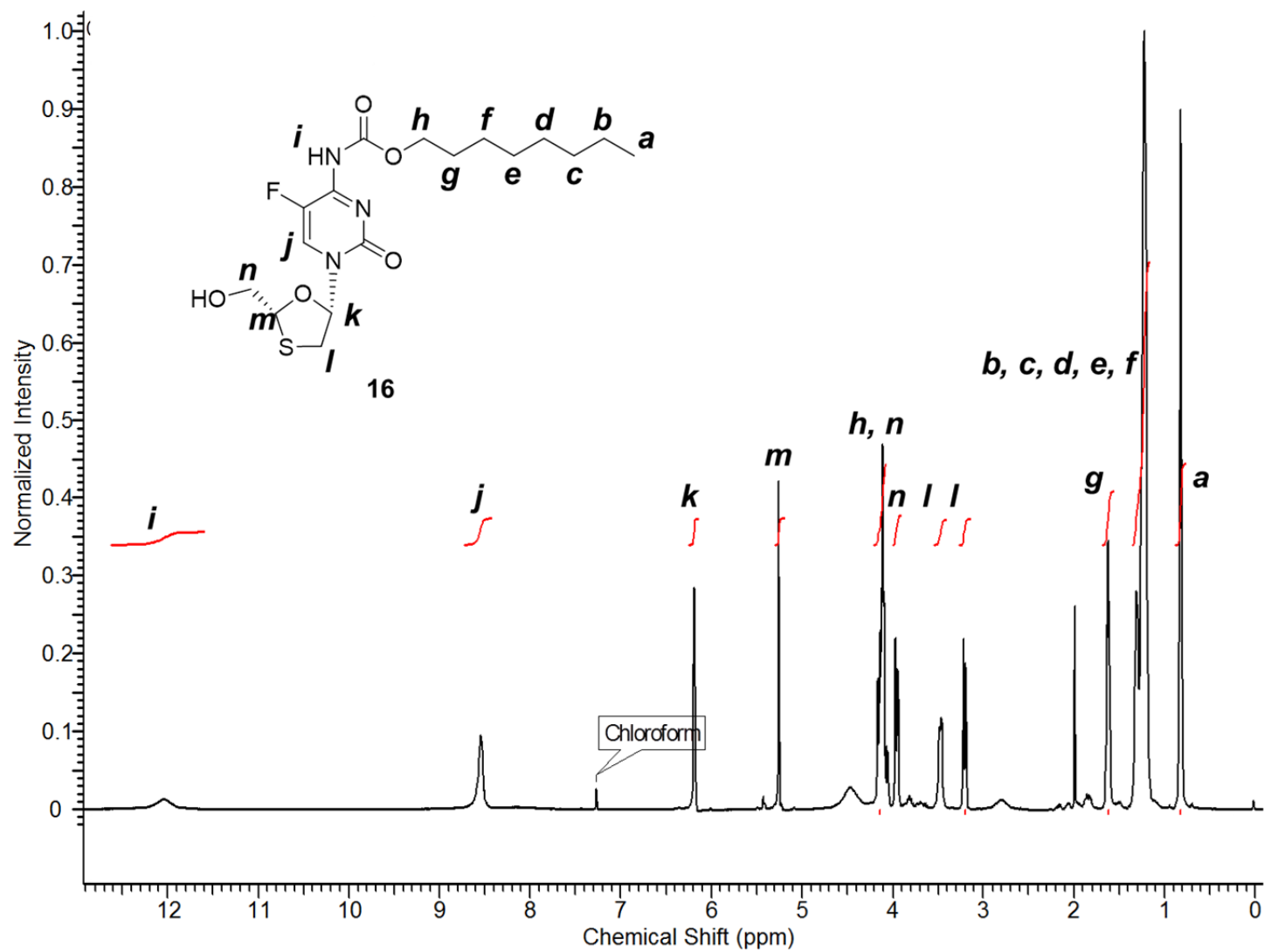
40 **Supplementary Figure 14.**  $^1\text{H}$  NMR (500 MHz) of **14** in  $\text{CDCl}_3$ .



41

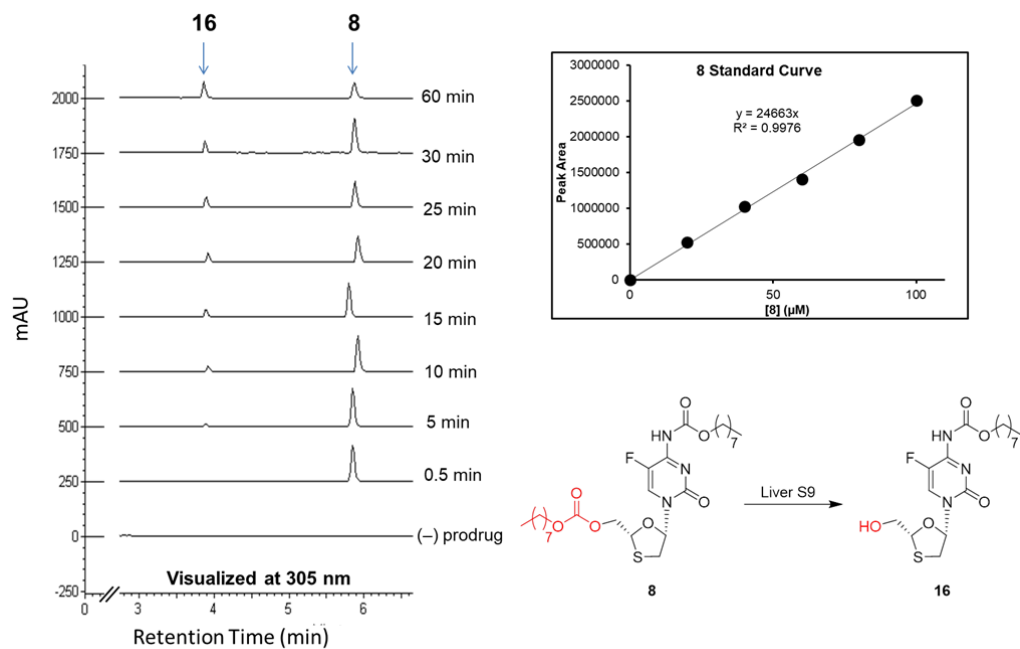
42 **Supplementary Figure 15.** <sup>1</sup>H NMR (500 MHz) of **15** in CDCl<sub>3</sub>.





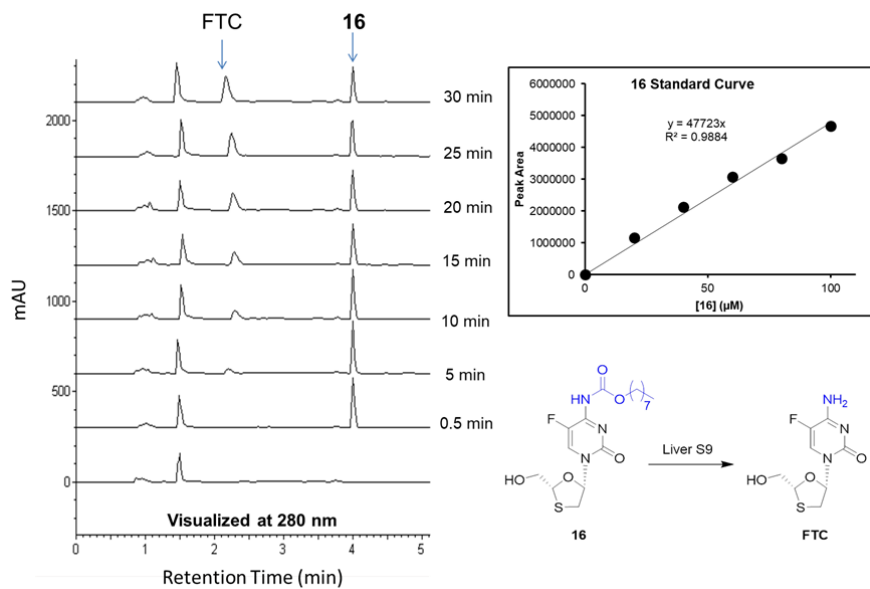
43

44 **Supplementary Figure 16.** <sup>1</sup>H NMR (500 MHz) of **16** in CDCl<sub>3</sub>



45

46 **Supplementary Figure 17.** Representative HPLC stackplot and standard curve at 305 nm  
 47 ( $\lambda_{\max}$  of FTC carbamates) showing cleavage of **8** to **16** in liver S9 fractions.



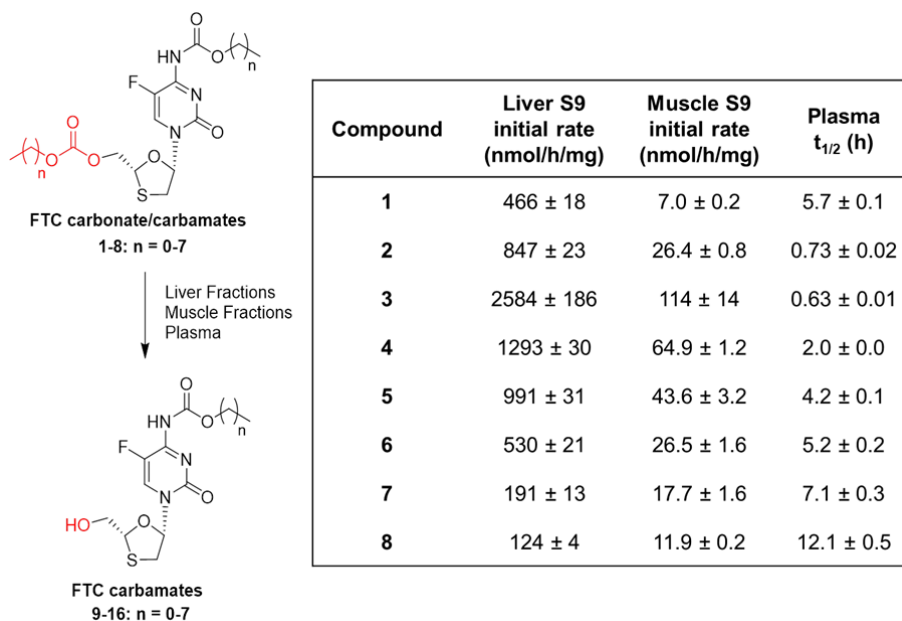
48

49 **Supplementary Figure 18.** Representative HPLC stackplot at 280 nm ( $\lambda_{\max}$  of FTC)  
 50 and standard curve at 305 nm ( $\lambda_{\max}$  of FTC carbamates) showing cleavage of **16** to **FTC** in liver  
 51 S9 fractions.

52

53

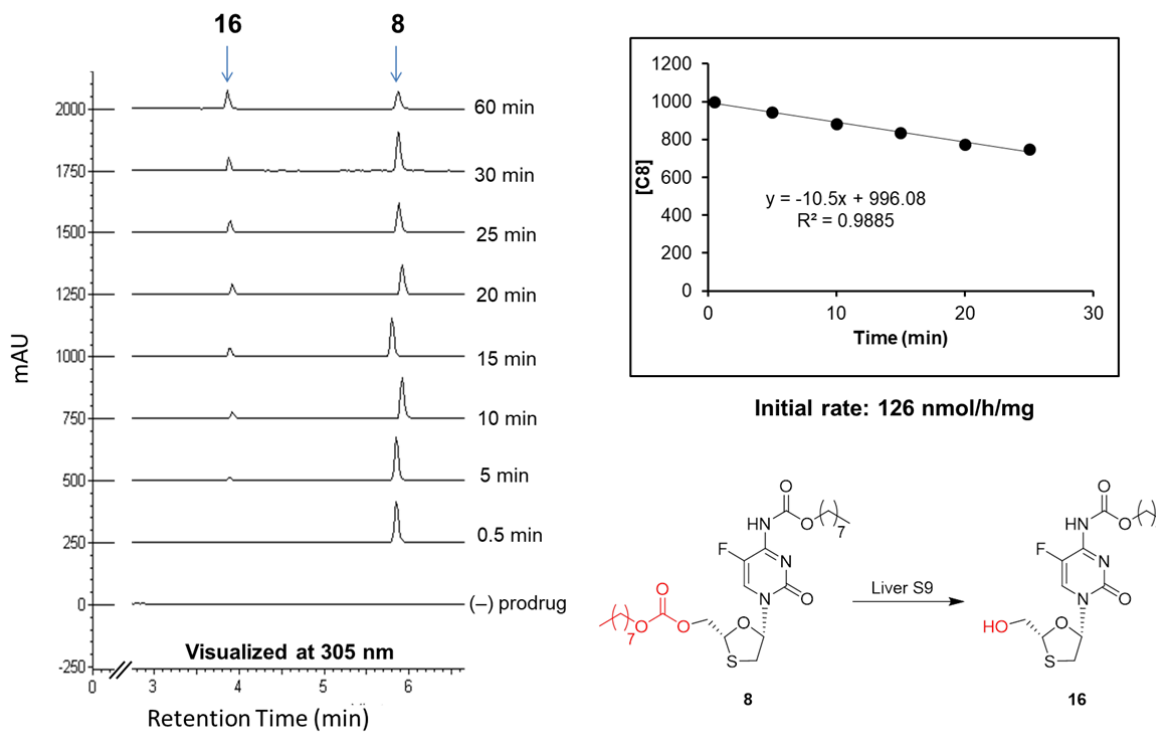
54



55

56 **Supplementary Figure 19.** Calculated initial rates (at 1 mM) of carbonate cleavage of **1-8** in  
 57 human liver and muscle S9 fractions, and half-lives in human plasma.

58

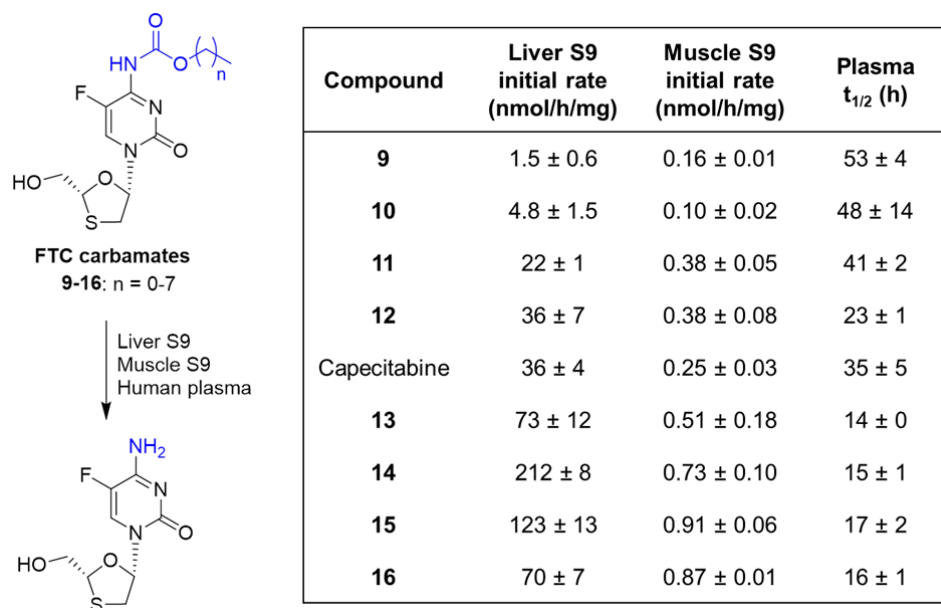


59

60 **Supplementary Figure 20.** Left: Representative HPLC stackplot at 305 nm ( $\lambda_{max}$  of FTC  
 61 carbamates) and calculated initial rate showing cleavage of **8** to **16** in liver S9 fractions.

62

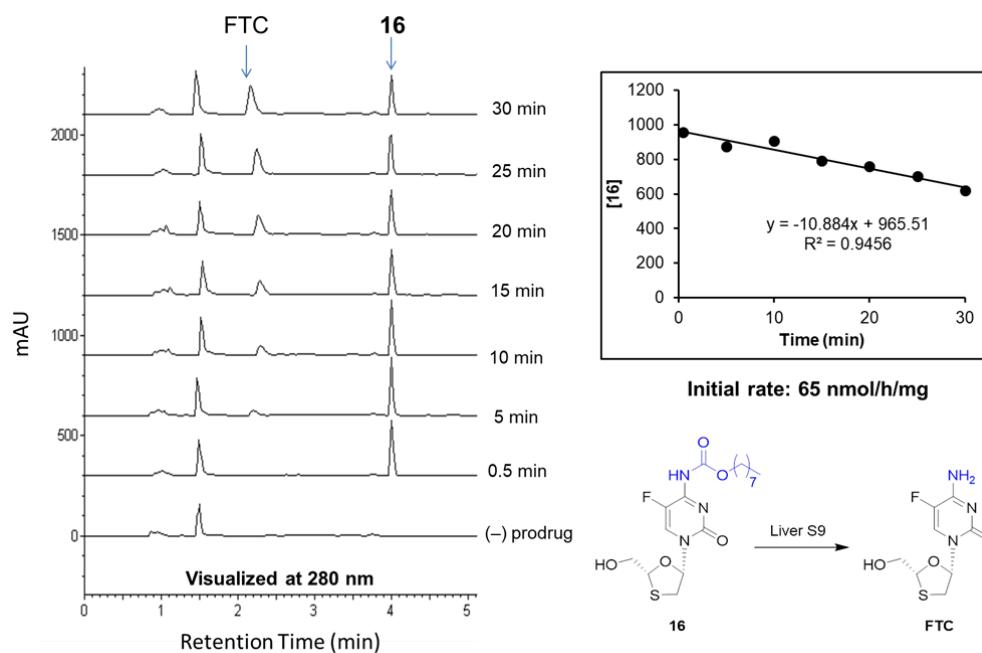
63



64

65 **Supplementary Figure 21.** Calculated initial rates (at 1 mM) of carbamate cleavage of **9-16**  
66 and capecitabine in human liver and muscle S9 fractions, and half-lives in human plasma.

67

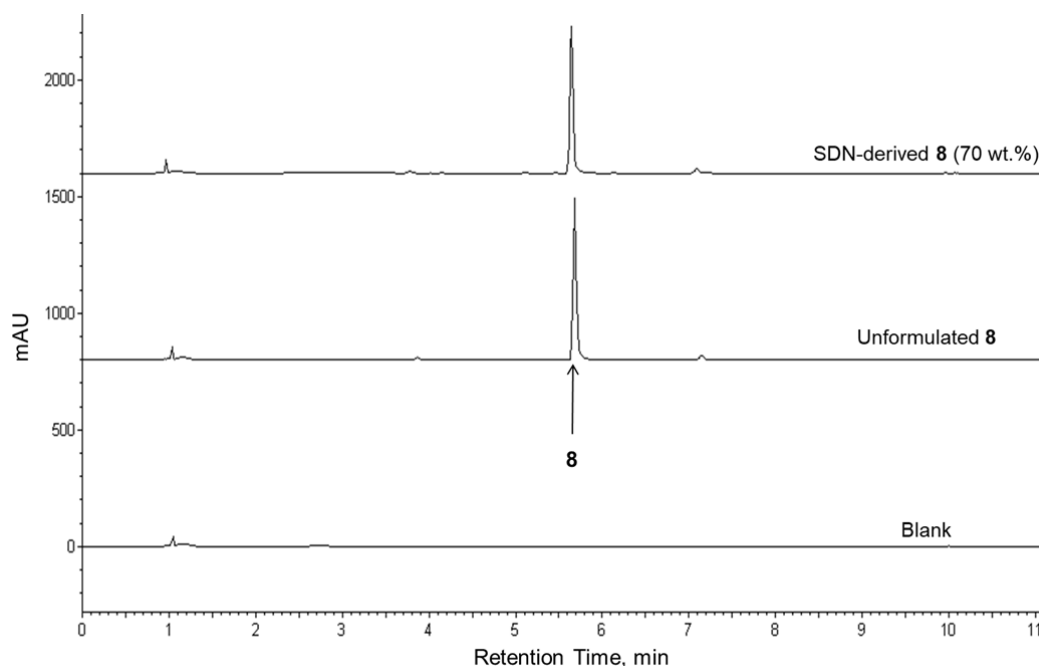


68

69 **Supplementary Figure 22.** Left: Representative HPLC stackplot at 280 nm ( $\lambda_{max}$  of FTC)  
70 and calculated initial rate showing cleavage of **16** to FTC in human liver S9 fractions.

71

72



73

74 **Supplementary Figure 23.** Representative HPLC stackplot at 305 nm ( $\lambda_{\text{max}}$  of FTC  
 75 carbamates) showing **8** derived from SSPNs relative to an unformulated prodrug control at  
 76 equal concentration.

77

78

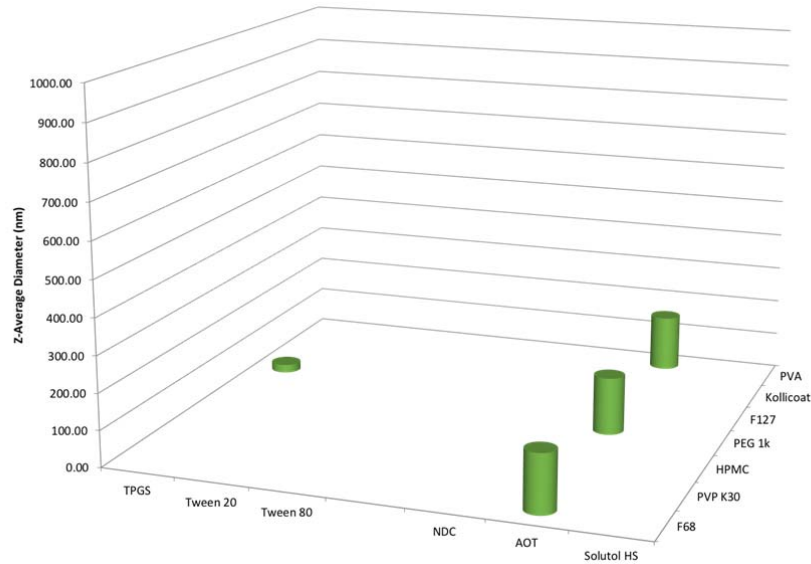
79

	F68	PVPk30	HPMC	PEG1K	F127	Kollocoat	PVA	Surfactant "Hits"
TPGS	5	3	4	1	4	2	3	22
Tween 20	4	8	6	5	4	5	6	38
Tween 80	4	4	4	4	7	3	6	32
NDC	6	8	9	7	5	7	6	48
AOT	6	5	5	6	6	4	5	37
Solutol	4	6	5	4	7	2	5	33
Polymer "Hits"	29	34	33	27	33	23	31	

80

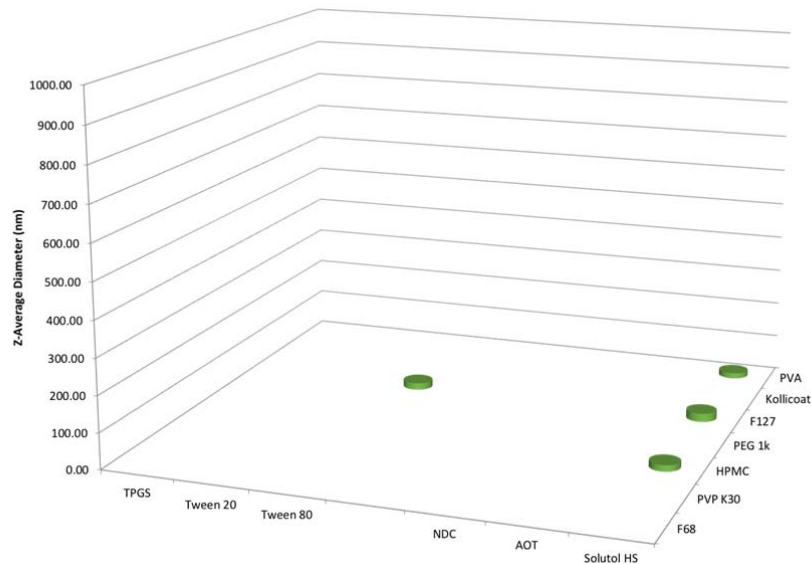
81 **Supplementary Figure 24.** The number of hits for each binary combination of polymer and  
 82 surfactant that occurred across the combined SSPN libraries at 10 wt% loading of prodrug.  
 83 The central cells indicate the number of times an exact combination appeared as a SSPN hit,  
 84 while the bottom and furthest right column show the total number of SSPN hits in which a  
 85 given single excipient appears.

86



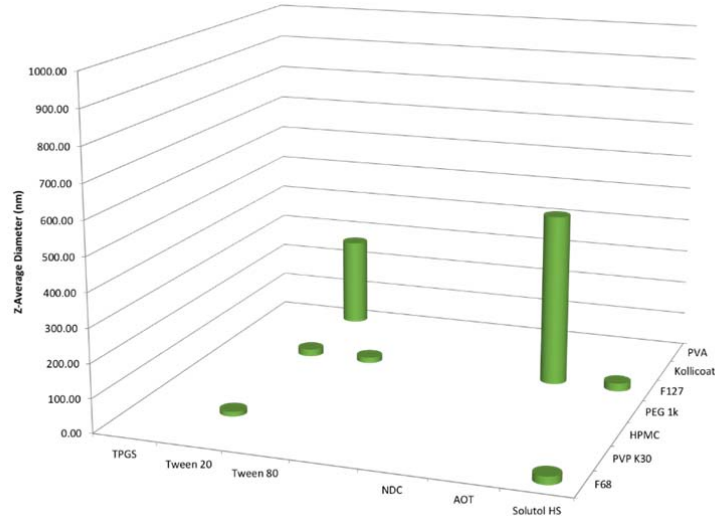
87

88 **Supplementary Figure 25.** Number of SSPN “hits” generated from a library of 42 binary  
 89 combinations of polymer and surfactant, with prodrug **1** at 10 wt% loading relative to  
 90 excipients. Data is shown as the average of 3 DLS scans for the z-average hydrodynamic  
 91 diameter, with only those determined as ‘hits’ being shown. A ‘hit’ was confirmed if re-  
 92 dispersion was easily achieved at 1 mg/mL, z-average diameter <1000nm, and  
 93 polydispersity index <0.4



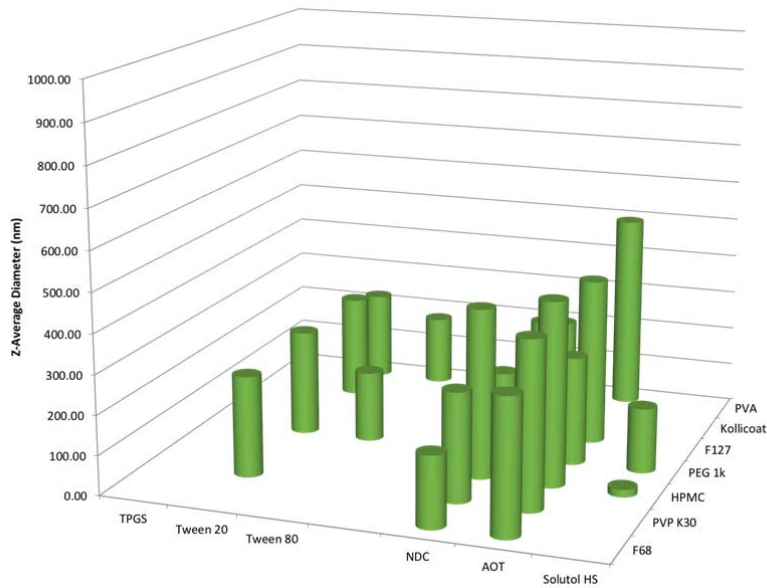
94

95 **Supplementary Figure 26.** Number of SSPN “hits” generated from a library of 42 binary  
 96 combinations of polymer and surfactant, with prodrug **2** at 10 wt% loading relative to  
 97 excipients. Data is shown as the average of 3 DLS scans for the z-average hydrodynamic  
 98 diameter, with only those determined as ‘hits’ being shown. A ‘hit’ was confirmed if re-  
 99 dispersion was easily achieved at 1 mg/mL, z-average diameter <1000nm, and  
 100 polydispersity index <0.4



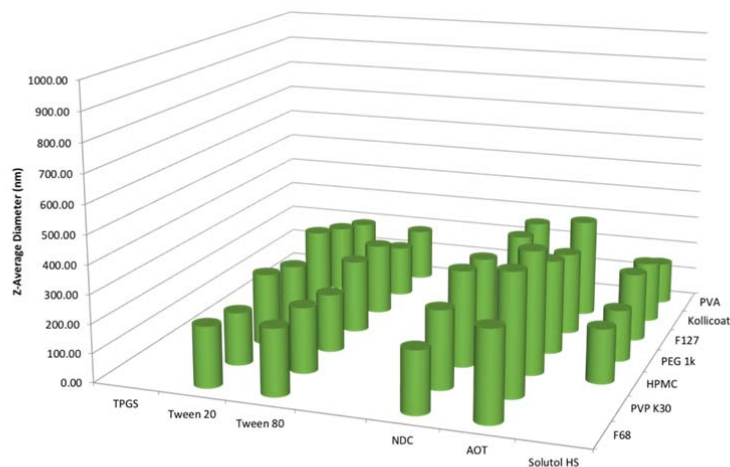
101

102 **Supplementary Figure 27.** Number of SSPN “hits” generated from a library of 42 binary  
 103 combinations of polymer and surfactant, with prodrug **3** at 10 wt% loading relative to  
 104 excipients. Data is shown as the average of 3 DLS scans for the z-average hydrodynamic  
 105 diameter, with only those determined as ‘hits’ being shown. A ‘hit’ was confirmed if re-  
 106 dispersion was easily achieved at 1 mg/mL, z-average diameter <1000nm, and  
 107 polydispersity index <0.4



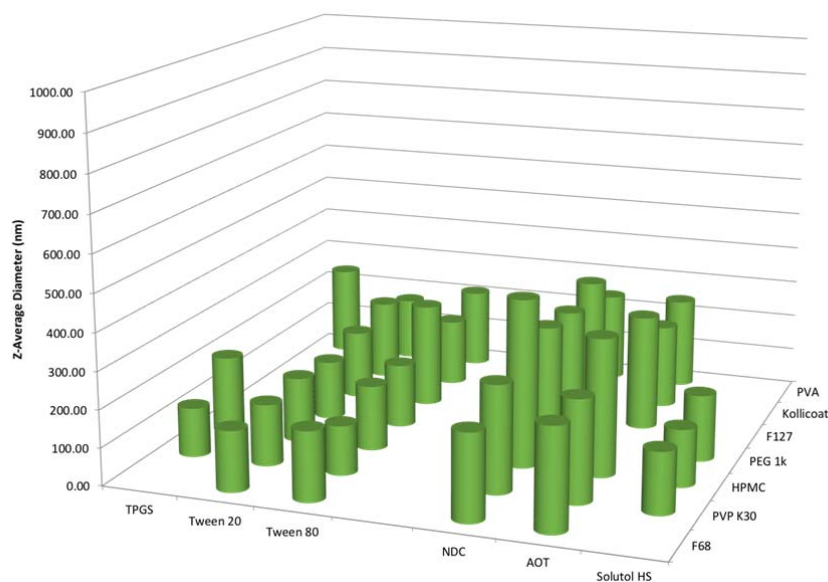
108

109 **Supplementary Figure 28.** Number of SSPN “hits” generated from a library of 42 binary  
 110 combinations of polymer and surfactant, with prodrug **4** at 10 wt% loading relative to  
 111 excipients. Data is shown as the average of 3 DLS scans for the z-average hydrodynamic  
 112 diameter, with only those determined as ‘hits’ being shown. A ‘hit’ was confirmed if re-  
 113 dispersion was easily achieved at 1 mg/mL, z-average diameter <1000nm, and  
 114 polydispersity index <0.4



115

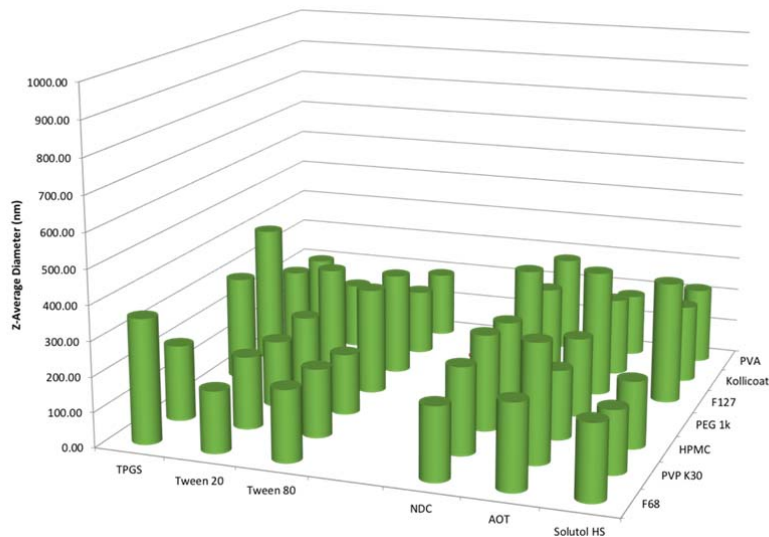
116 **Supplementary Figure 29.** Number of SSPN “hits” generated from a library of 42 binary  
 117 combinations of polymer and surfactant, with prodrug **5** at 10 wt% loading relative to  
 118 excipients. Data is shown as the average of 3 DLS scans for the z-average hydrodynamic  
 119 diameter, with only those determined as ‘hits’ being shown. A ‘hit’ was confirmed if re-  
 120 dispersion was easily achieved at 1 mg/mL, z-average diameter <1000nm, and  
 121 polydispersity index <0.4



122

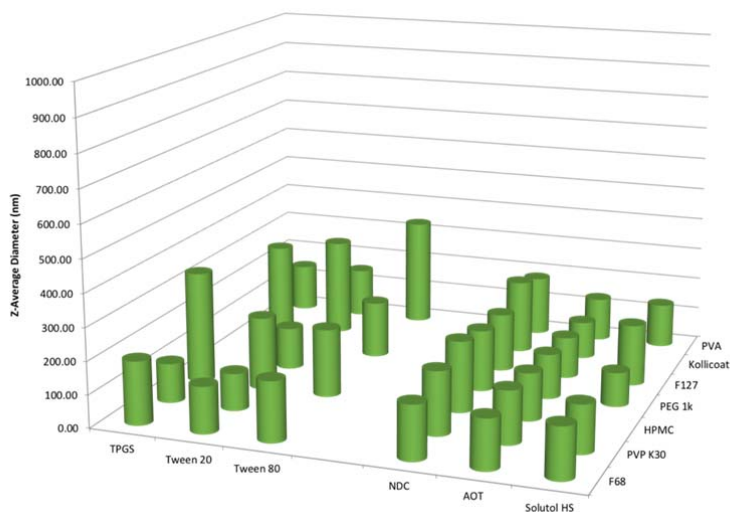
123 **Supplementary Figure 30.** Number of SSPN “hits” generated from a library of 42 binary  
 124 combinations of polymer and surfactant, with prodrug **6** at 10 wt% loading relative to  
 125 excipients. Data is shown as the average of 3 DLS scans for the z-average hydrodynamic  
 126 diameter, with only those determined as ‘hits’ being shown. A ‘hit’ was confirmed if re-  
 127 dispersion was easily achieved at 1 mg/mL, z-average diameter <1000nm, and  
 128 polydispersity index <0.4





129

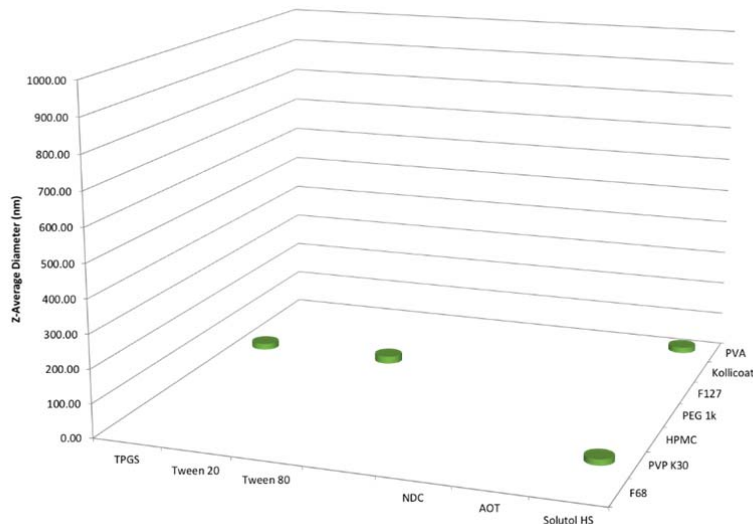
130 **Supplementary Figure 31.** Number of SSPN “hits” generated from a library of 42 binary  
 131 combinations of polymer and surfactant, with prodrug **7** at 10 wt% loading relative to  
 132 excipients. Data is shown as the average of 3 DLS scans for the z-average hydrodynamic  
 133 diameter, with only those determined as ‘hits’ being shown. A ‘hit’ was confirmed if re-  
 134 dispersion was easily achieved at 1 mg/mL, z-average diameter <1000nm, and  
 135 polydispersity index <0.4



136

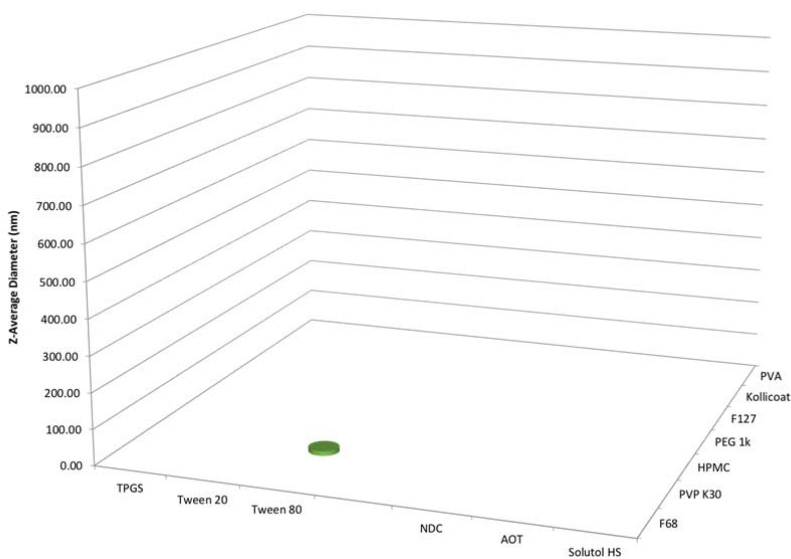
137 **Supplementary Figure 32.** Number of SSPN “hits” generated from a library of 42 binary  
 138 combinations of polymer and surfactant, with prodrug **8** at 10 wt% loading relative to  
 139 excipients. Data is shown as the average of 3 DLS scans for the z-average hydrodynamic  
 140 diameter, with only those determined as ‘hits’ being shown. A ‘hit’ was confirmed if re-  
 141 dispersion was easily achieved at 1 mg/mL, z-average diameter <1000nm, and  
 142 polydispersity index <0.4

143



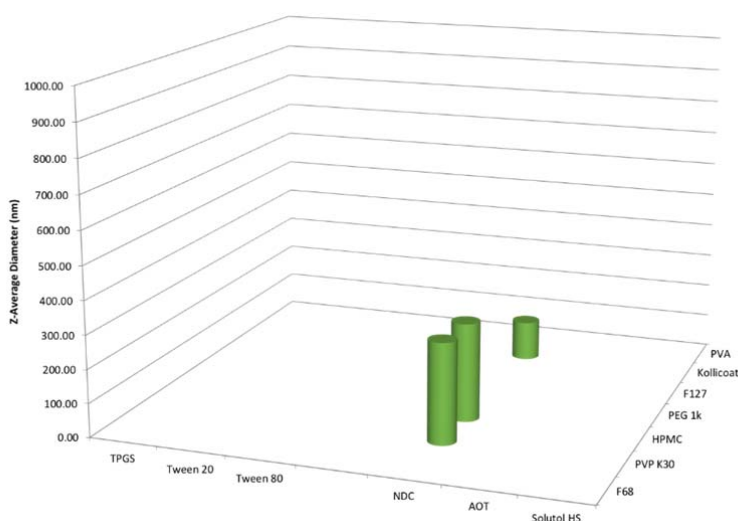
144

145 **Supplementary Figure 33.** Number of SSPN “hits” generated from a library of 42 binary  
 146 combinations of polymer and surfactant, with prodrug **10** at 10 wt% loading relative to  
 147 excipients. Data is shown as the average of 3 DLS scans for the z-average hydrodynamic  
 148 diameter, with only those determined as ‘hits’ being shown. A ‘hit’ was confirmed if re-  
 149 dispersion was easily achieved at 1 mg/mL, z-average diameter <1000nm, and  
 150 polydispersity index <0.4



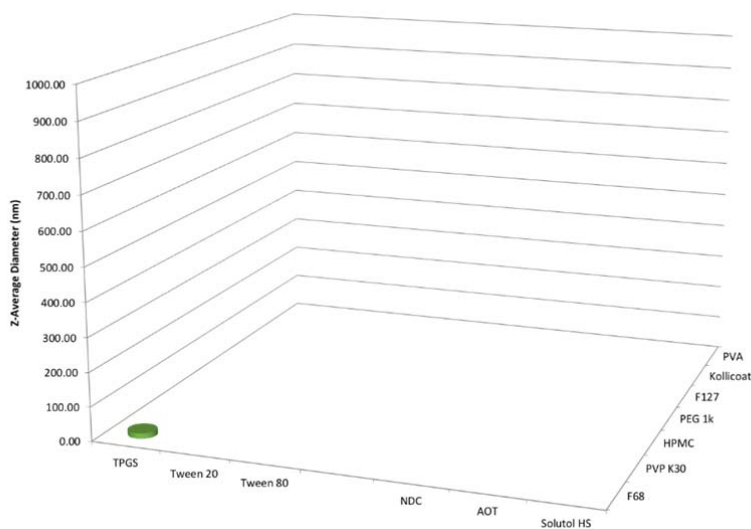
151

152 **Supplementary Figure 34.** Number of SSPN “hits” generated from a library of 42 binary  
 153 combinations of polymer and surfactant, with prodrug **11** at 10 wt% loading relative to  
 154 excipients. Data is shown as the average of 3 DLS scans for the z-average hydrodynamic  
 155 diameter, with only those determined as ‘hits’ being shown. A ‘hit’ was confirmed if re-  
 156 dispersion was easily achieved at 1 mg/mL, z-average diameter <1000nm, and  
 157 polydispersity index <0.4



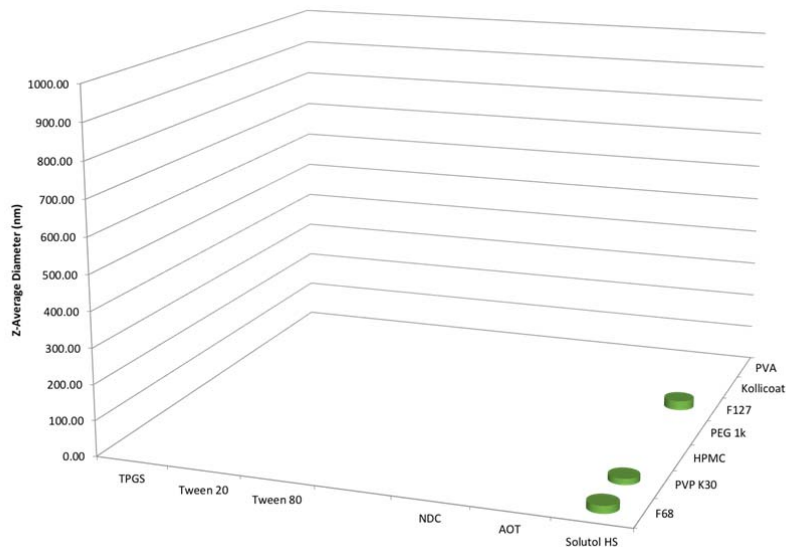
159

160 **Supplementary Figure 35.** Number of SSPN “hits” generated from a library of 42 binary  
 161 combinations of polymer and surfactant, with prodrug **13** at 10 wt% loading relative to  
 162 excipients. Data is shown as the average of 3 DLS scans for the z-average hydrodynamic  
 163 diameter, with only those determined as ‘hits’ being shown. A ‘hit’ was confirmed if re-  
 164 dispersion was easily achieved at 1 mg/mL, z-average diameter <1000nm, and  
 165 polydispersity index <0.4



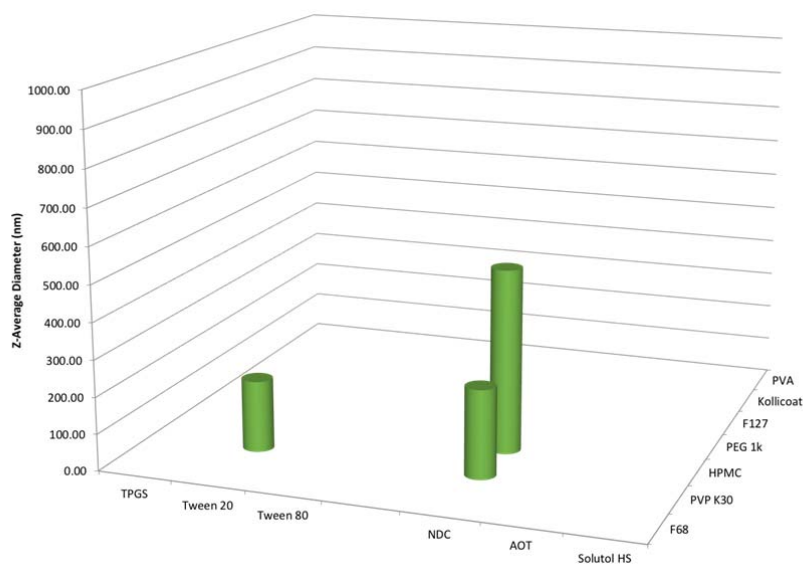
166

167 **Supplementary Figure 36.** Number of SSPN “hits” generated from a library of 42 binary  
 168 combinations of polymer and surfactant, with prodrug **14** at 10 wt% loading relative to  
 169 excipients. Data is shown as the average of 3 DLS scans for the z-average hydrodynamic  
 170 diameter, with only those determined as ‘hits’ being shown. A ‘hit’ was confirmed if re-  
 171 dispersion was easily achieved at 1 mg/mL, z-average diameter <1000nm, and  
 172 polydispersity index <0.4



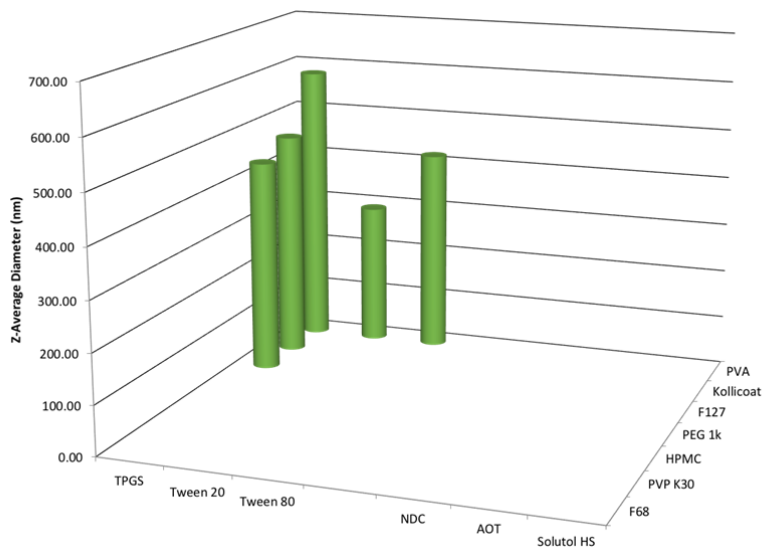
173

174 **Supplementary Figure 37.** Number of SSPN “hits” generated from a library of 42 binary  
 175 combinations of polymer and surfactant, with prodrug **15** at 10 wt% loading relative to  
 176 excipients. Data is shown as the average of 3 DLS scans for the z-average hydrodynamic  
 177 diameter, with only those determined as ‘hits’ being shown. A ‘hit’ was confirmed if re-  
 178 dispersion was easily achieved at 1 mg/mL, z-average diameter <1000nm, and  
 179 polydispersity index <0.4



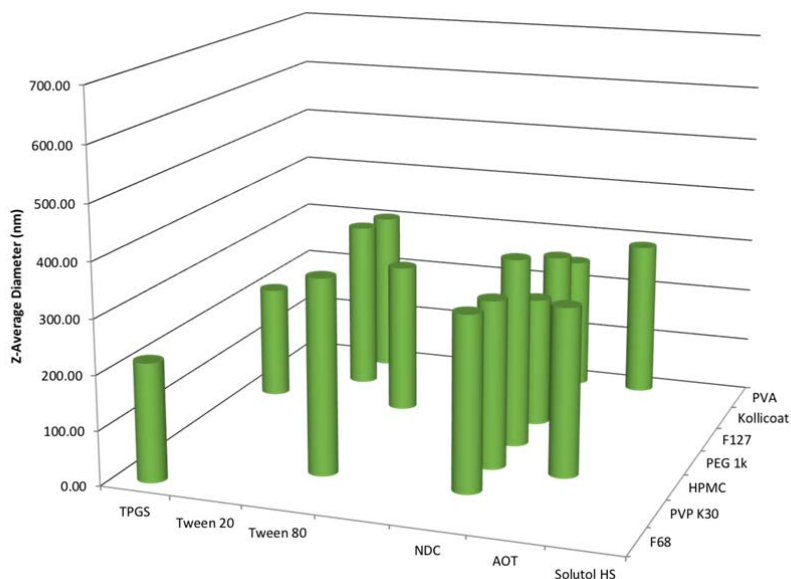
180

181 **Supplementary Figure 38.** Number of SSPN “hits” generated from a library of 42 binary  
 182 combinations of polymer and surfactant, with prodrug **16** at 10 wt% loading relative to  
 183 excipients. Data is shown as the average of 3 DLS scans for the z-average hydrodynamic  
 184 diameter, with only those determined as ‘hits’ being shown. A ‘hit’ was confirmed if re-  
 185 dispersion was easily achieved at 1 mg/mL, z-average diameter <1000nm, and  
 186 polydispersity index <0.4



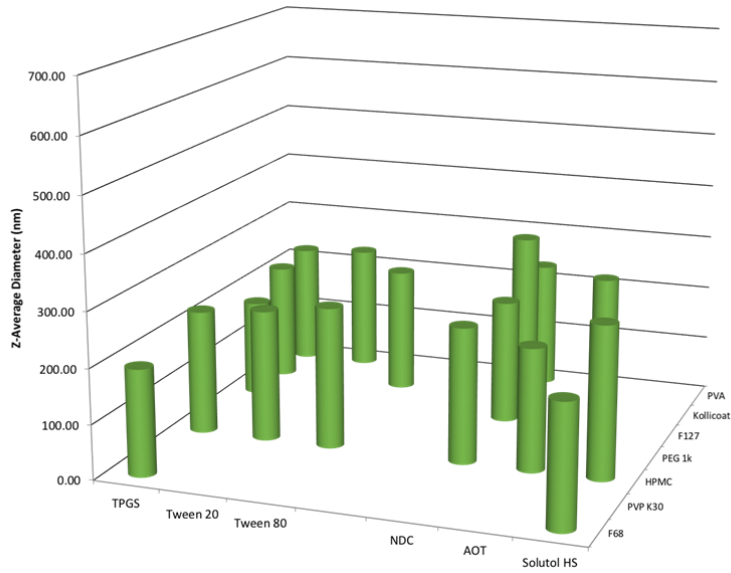
187

188 **Supplementary Figure 39.** Number of SSPN “hits” generated from a library of 42 binary  
 189 combinations of polymer and surfactant, with prodrug **4** at 50 wt% loading relative to  
 190 excipients. Data is shown as the average of 3 DLS scans for the z-average hydrodynamic  
 191 diameter, with only those determined as ‘hits’ being shown. A ‘hit’ was confirmed if re-  
 192 dispersion was easily achieved at 1 mg/mL, z-average diameter <1000nm, and  
 193 polydispersity index <0.4



194

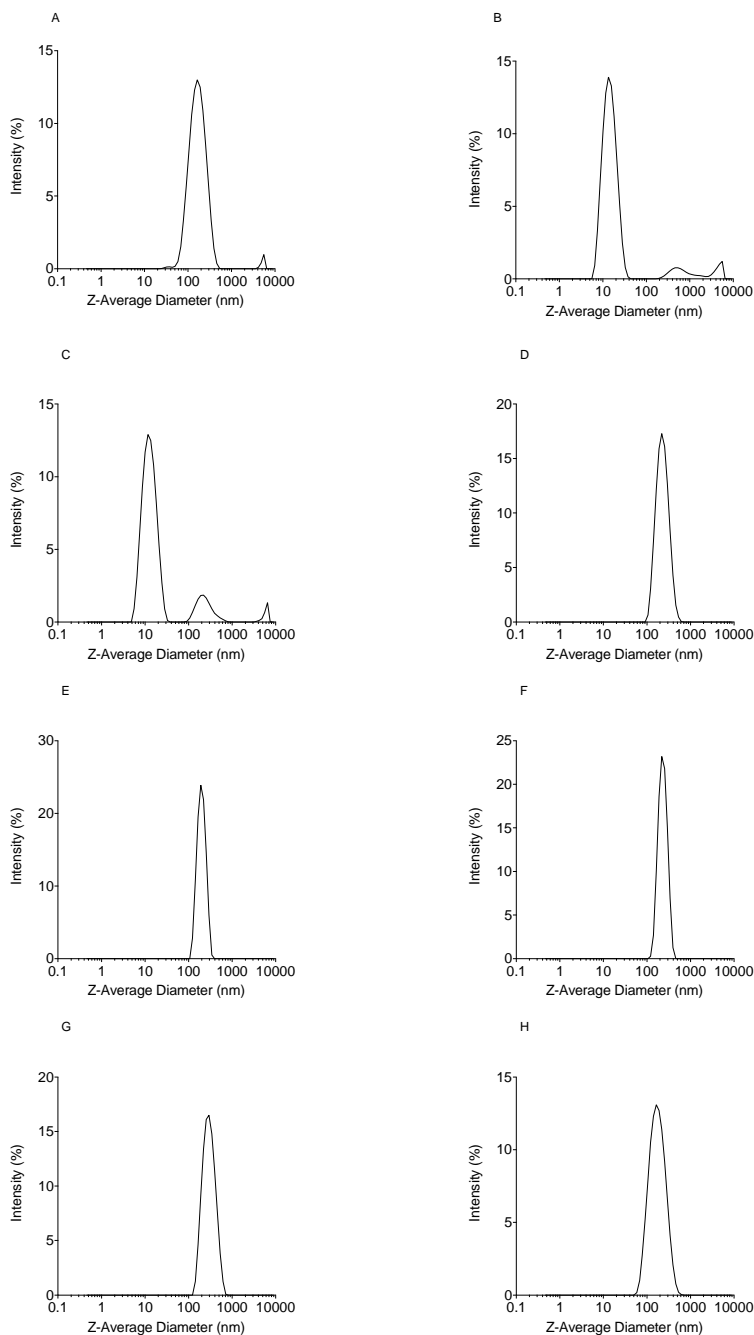
195 **Supplementary Figure 40.** Number of SSPN “hits” generated from a library of 42 binary  
 196 combinations of polymer and surfactant, with prodrug **6** at 50 wt% loading relative to  
 197 excipients. Data is shown as the average of 3 DLS scans for the z-average hydrodynamic  
 198 diameter, with only those determined as ‘hits’ being shown. A ‘hit’ was confirmed if re-  
 199 dispersion was easily achieved at 1 mg/mL, z-average diameter <1000nm, and  
 200 polydispersity index <0.4



201

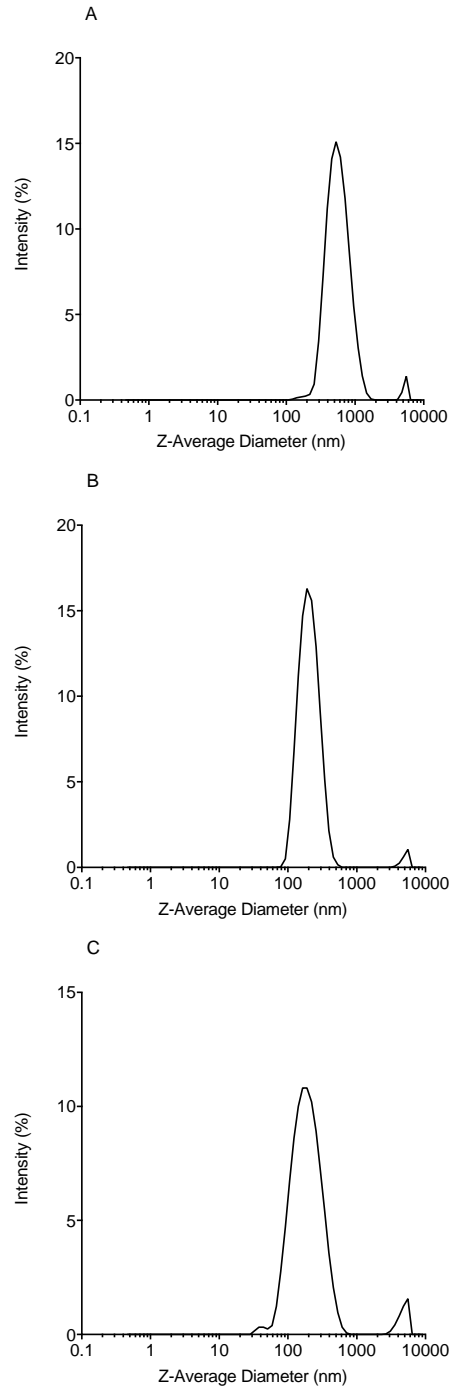
202 **Supplementary Figure 41.** Number of SSPN “hits” generated from a library of 42 binary  
 203 combinations of polymer and surfactant, with prodrug **8** at 50 wt% loading relative to  
 204 excipients. Data is shown as the average of 3 DLS scans for the z-average hydrodynamic  
 205 diameter, with only those determined as ‘hits’ being shown. A ‘hit’ was confirmed if re-  
 206 dispersion was easily achieved at 1 mg/mL, z-average diameter <1000nm, and  
 207 polydispersity index <0.4

208



209

210 **Supplementary Figure 42.** Representative Z-Average diameter particle size distribution of  
 211 selected hits from libraries of 10 wt% loaded SSPNs. Prodrug **1** stabilised by NDC+PVA (a),  
 212 prodrug **2** stabilised by Solutol + PVA (b), prodrug **3** stabilised by Tween 80 + PVPK30 (c),  
 213 prodrug **4** stabilised by AOT + PEG1K (d), prodrug **5** stabilised by Tween 20 + PVA (e),  
 214 prodrug **6** stabilised by NDC + Kollicoat (f), prodrug **7** stabilised by AOT + PVA, and  
 215 prodrug **8** stabilised by TPGS and PVA. Data is shown as the average of 3 scans from  
 216 dynamic light scattering analysis.

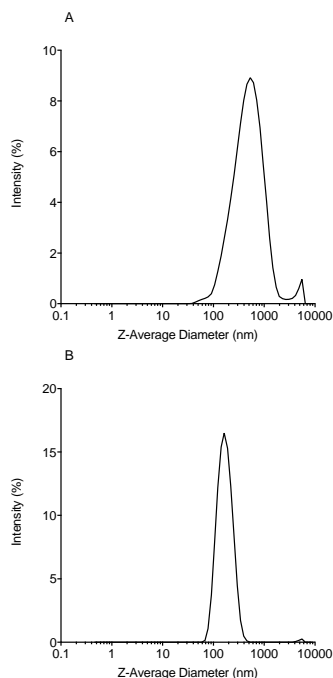


217

218 **Supplementary Figure 43.** Representative Z-Average diameter particle size distribution of  
 219 selected hits from libraries of 50 wt% loaded SSPNs. Prodrug **4** stabilised by TPGS +PVA  
 220 (a), prodrug **6** stabilised by TPGS + F127 (b), and prodrug **8** stabilised by TPGS + F127 (c).  
 221 Data is shown as the average of 3 scans from dynamic light scattering analysis.

222

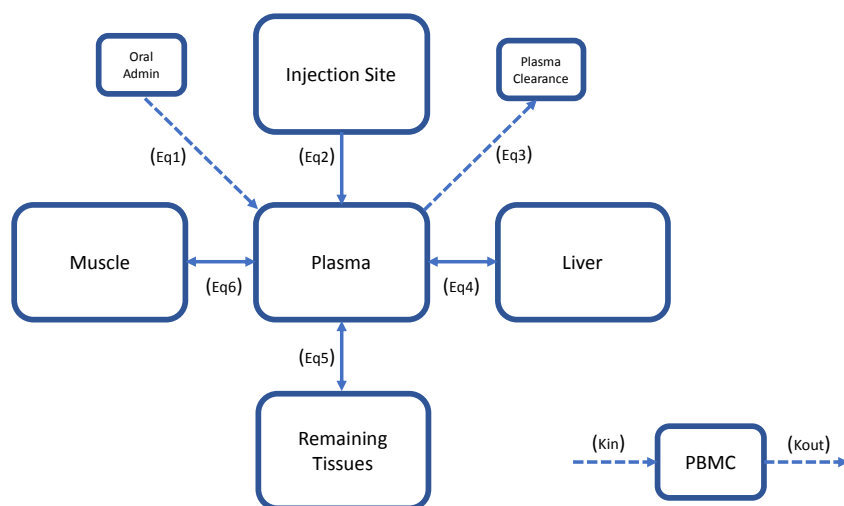




223

224 **Supplementary Figure 44.** Representative Z-Average diameter particle size distribution of  
 225 selected hits from libraries of 70 wt% loaded SSPNs. Prodrug **4** stabilised by Tween 20  
 226 +PVA (a) and prodrug **6** stabilised by AOT + PEG1K (b). Data is shown as the average of 3  
 227 scans from dynamic light scattering analysis.

228



229

230 **Supplementary Figure 45.** Diagram of the IVIVE model describing the systemic  
 231 distribution of carbonate/carbamate prodrugs, carbamate intermediary and FTC following  
 232 simulated IM injection. Also shown is the compartments for simulated oral administration  
 233 and clearance from the plasma. All numbers refer to equations used to describe the flow  
 234 between compartments. Also shown is the additional module to simulate intracellular FTC-  
 235 TP concentrations.

236

237

238 **Supplementary Table 1.** Measured retention times for **1-16**, **FTC**, and **Capecitabine** via the  
 239 RP-HPLC method described above: 0% to 100% solvent B over 5 minutes at a flow rate of 3  
 240 mL min<sup>-1</sup> (solvent A: Et<sub>3</sub>NHOAc (50 mM, pH 8), solvent B: acetonitrile. For prodrugs **1-8**  
 241 and **9-16**, retention time increases as carbon chain length increases, demonstrating an increase  
 242 in lipophilicity.

Compound	RP-HPLC Retention Time (min.)
<b>FTC</b>	2.2
<b>1</b>	3.0
<b>2</b>	3.4
<b>3</b>	3.7
<b>4</b>	4.2
<b>5</b>	4.6
<b>6</b>	5.1
<b>7</b>	5.4
<b>8</b>	5.9
<b>9</b>	2.7
<b>10</b>	2.9
<b>11</b>	3.0
<b>12</b>	3.2
<b>Capecitabine</b>	3.2
<b>13</b>	3.5
<b>14</b>	3.5
<b>15</b>	3.8
<b>16</b>	4.0

243

244 **Supplementary Table 2.** Excipients used to generate libraries of SSPNs consisting of 7  
 245 different polymers and 6 different surfactants, resulting in 42 individual binary combinations

Polymer	Surfactant
Polyethylene glycol 1000 (PEG1K)	Polysorbate 20 (Tween 20)
Polyvinylpyrrolidone K30 (PVPK30)	Polysorbate 80 (Tween 80)
Polyoxyethylene-polyoxypropylene block copolymer (Pluronic F68)	Sodium deoxycholate (NDC)
Polyoxyethylene-polyoxypropylene block copolymer (Pluronic F127)	D- $\alpha$ -Tocopherol polyethylene glycol 1000 succinate (TPGS)
Polyvinyl alcohol (PVA)	Diocetyl sulfosuccinate sodium salt (AOT)
Polyvinyl alcohol-polyethylene glycol copolymer and polyvinyl alcohol (Kollicoat Protect)	Polyethylene glycol (15)-hydroxystearate (Solutol)
Hydroxypropyl methylcellulose (HPMC)	

246

247

248 **Supplementary Table 3.** Reproducibility of selected SSPN synthesis (varying formulations)  
 249 with drug loading  $\geq 50$  wt% (n=3)

Pro Drug	Drug Loading (wt%)	Polymer	Surfactant	Z-average nm (+/-SD)	PDI (+/- SD)
8	70	F127	TPGS	267 (26)	0.314 (0.022)
4	50	F127	TPGS	702 (111)	0.305 (0.090)
4	50	PVA	Tween 20	782 (199)	0.450 (0.152)
6	50	F127	TPGS	239 (50)	0.323 (0.042)
6	50	PVA	Tween 20	298 (21)	0.339 (0.038)
6	50	HPMC	NDC	261 (44)	0.295 (0.019)
6	50	HPMC	AOT	293 (9)	0.294 (0.028)
8	50	F127	TPGS	196 (6)	0.345 (0.027)
8	50	PVA	Tween 20	261 (17)	0.376 (0.038)
8	50	HPMC	NDC	217 (10)	0.306 (0.022)
8	50	HPMC	AOT	237 (5)	0.296 (0.021)

250

251 **Supplementary Table 4.** Table showing the key parameters used in simulating the systemic  
 252 distribution of carbonate/carbamate prodrugs, carbamate intermediary and FTC following  
 253 simulated IM injection.

	FTC	C4 carbamate carbonate	C4 carbamate	C8 carbamate carbonate	C8 carbamate
Molecular Weight	247.45	447.49	347.37	559.69	403.47
Hydrolysis liver ( $h^{-1}$ )		0.5786	0.0125	0.0694	0.0282
Hydrolysis muscle ( $h^{-1}$ )		0.0290	0.001	0.0067	0.004
Hydrolysis plasma ( $h^{-1}$ )		1.4	16.0	8.4	11.1
Plasma Cl (L/h)	19.35	19.35	19.35	19.35	19.35
Release Rate ( $h^{-1}$ )		0.0015		0.0015	
Liver to plasma ratio	0.8	6.1	1.0	5.5	5.4
Muscle to plasma ratio	0.8	3.2	0.9	3.3	3.4
Tissue (per) to plasma ratio	0.7	8.2	1.1	4.7	4.4

254

255

256 **Supplementary Table 5.** Pharmacokinetic parameters following oral administration  
 257 (simulated and observed values) of 400mg FTC at steady state. Values represent mean  
 258 (minimum and maximum values).

	Simulated	Observed
Cmax (ng/mL)	4666 (3461-6774)	2968 (1582-4165)
Cmin (ng/mL)	57 (1-158)	63 (48-134)
AUC (ng/h/mL)	29052 (27674-29524)	16484 (11524-21388)
IC Cmax (fmol/ $10^6$ cells)	1264 (370-2384)	
IC Cmin (fmol/ $10^6$ cells)	126 (48-206)	

259

260 **Supplementary Table 6.** Simulated pharmacokinetic parameters following: IM injection of  
 261 SSPN containing C4 prodrug. Values represent mean ( $\pm$  standard deviation).

	FTC	Carbamate carbonate	Carbamate
Cmax (ng/mL)	97 ( $\pm$ 21.23)	0.5 ( $\pm$ 1.45)	46.5 ( $\pm$ 11.90)
Cmin (ng/mL)	34.9 ( $\pm$ 7.68)	0.2 ( $\pm$ 0.50)	16.3 ( $\pm$ 4.26)
AUC (ng/h/mL)	44275.1 ( $\pm$ 9754.70)	214.7 ( $\pm$ 642.95)	20869.7 (5427.37)
IC Cmax (fmol/10 <sup>6</sup> cells)	618.8 (302.48)		
IC Cmin (fmol/10 <sup>6</sup> cells)	433.1 ( $\pm$ 211.06)		

262

263 **Supplementary Table 7.** Simulated pharmacokinetic parameters following: IM injection of  
 264 SSPN containing C8 prodrug. Values represent mean ( $\pm$  standard deviation).

	FTC	Carbamate carbonate	Carbamate
Cmax (ng/mL)	146.4 ( $\pm$ 19.44)	2.2 ( $\pm$ 4.44)	15.3 ( $\pm$ 7.44)
Cmin (ng/mL)	52.4 (6.81)	0.8 (1.64)	5.4 ( $\pm$ 2.72)
AUC (ng/h/mL)	66643.9 ( $\pm$ 8747.28)	988.0 ( $\pm$ 2090.69)	6839.5 ( $\pm$ 3446.55)
IC Cmax (fmol/10 <sup>6</sup> cells)	921.2 ( $\pm$ 391.40)		
IC Cmin (fmol/10 <sup>6</sup> cells)	644.5 ( $\pm$ 270.39)		

265

266

267 **Supplementary Table 8.** Table showing the key parameters used for the ad hoc model  
 268 (model 2) in simulating the systemic distribution of carbonate/carbamate prodrugs, carbamate  
 269 intermediary and FTC following simulated IM injection.

	FTC	C4 carbamate carbonate	C4 carbamate	C8 carbamate carbonate	C8 carbamate
Ka (h <sup>-1</sup> )	0.9				
Molecular Weight	247.45	447.49	347.37	559.69	403.47
Hydrolysis liver (h <sup>-1</sup> )		0.5786	0.0125	0.0694	0.0282
Hydrolysis muscle (h <sup>-1</sup> )		0.0290	0.001	0.0067	0.004
Hydrolysis plasma (h <sup>-1</sup> )		1.4	16.0	8.4	11.1
Plasma Cl (L/h)	24.5	24.5	24.5	24.5	24.5
Release Rate (h <sup>-1</sup> )		0.0015		0.0015	
Liver to plasma ratio	0.8	6.1	1.0	5.5	5.4
Muscle to plasma ratio	0.8	3.2	0.9	3.3	3.4
Tissue (per) to plasma ratio	1.2	8.2	1.1	4.7	4.4

270

271

272

273 **Supplementary Table 9.** Pharmacokinetic parameters following oral administration  
 274 (simulated and observed values) of 400mg FTC at steady state. Observed values represent  
 275 average values from 3 independent clinical studies. Values represent mean ( $\pm$  standard  
 276 deviation).

	Simulated	Observed
Cmax (ng/mL)	1857 ( $\pm$ 333.9)	1773 ( $\pm$ 46.1)
Cmin (ng/mL)	36 ( $\pm$ 32.5)	67 ( $\pm$ 25)
AUC (ng/h/mL)	13827 ( $\pm$ 1808.4)	9100 ( $\pm$ 1646)
IC Cmax (fmol/10 <sup>6</sup> cells)	3081 ( $\pm$ 1128.9)	
IC Cmin (fmol/10 <sup>6</sup> cells)	2676 ( $\pm$ 994.5)	

277

278

279 **Supplementary Table 10.** Simulated pharmacokinetic parameters following: IM injection of  
 280 SSPN containing C4 prodrug. Values represent mean ( $\pm$  standard deviation).

	FTC	Carbamate carbonate	Carbamate
Cmax (ng/mL)	75 ( $\pm$ 19.8)	0.2 ( $\pm$ 0.19)	39 ( $\pm$ 10.7)
Cmin (ng/mL)	28 ( $\pm$ 7.8)	0.1 ( $\pm$ 0.07)	15 ( $\pm$ 4.1)
AUC (ng/h/mL)	32949 ( $\pm$ 8856.5)	81 ( $\pm$ 80.1)	17291 ( $\pm$ 4649.1)
IC Cmax (fmol/10 <sup>6</sup> cells)	439 ( $\pm$ 176.0)		
IC Cmin (fmol/10 <sup>6</sup> cells)	332 ( $\pm$ 132.3)		

281

282

283 **Supplementary Table 11.** Simulated pharmacokinetic parameters following: IM injection of  
 284 SSPN containing C8 prodrug. Values represent mean ( $\pm$  standard deviation).

	FTC	Carbamate carbonate	Carbamate
Cmax (ng/mL)	101 ( $\pm$ 26.8)	1 ( $\pm$ 1.8)	23 ( $\pm$ 12.3)
Cmin (ng/mL)	39 ( $\pm$ 10.6)	0.5 ( $\pm$ 0.70)	8 ( $\pm$ 4.7)
AUC (ng/h/mL)	44394 ( $\pm$ 11929.7)	523 ( $\pm$ 798.0)	9882 ( $\pm$ 5352.1)
IC Cmax (fmol/10 <sup>6</sup> cells)	608 ( $\pm$ 286.4)		
IC Cmin (fmol/10 <sup>6</sup> cells)	444 ( $\pm$ 197.1)		

285

286

287

288

289

## Supplementary Methods

290

291 **HPLC method for analysis of prodrug cleavage:** Kinetic analysis of prodrug cleavage was  
292 performed on a Beckman Gold Nouveau System Gold HPLC using a C<sub>18</sub> column (Grace  
293 Altima, 3 μm C<sub>18</sub> analytical Rocket® column, 53 mm × 7 mm). All HPLC analyses were  
294 performed using the following method: 0% to 100% solvent B over 5 minutes at a flow rate  
295 of 3 mL min<sup>-1</sup> (solvent A: Et<sub>3</sub>NHOAc (50 mM, pH 8), solvent B: acetonitrile), which  
296 provided adequate separation between the prodrug and observed products. Prodrug  
297 concentration was determined by comparison to standard curves acquired at the identified  
298 λ<sub>max</sub> of 305 nm. The identity of product peaks was confirmed by comparison of retention  
299 times and UV profiles to those of authentic standards. The products of hydrolysis of prodrugs  
300 **1-8** (λ<sub>max</sub> = 305 nm) are carbamate prodrugs **9-16** (λ<sub>max</sub> = 305 nm), which reproducibly appear  
301 with shorter retention times compared to the corresponding carbonate/carbamate prodrugs.  
302 The product of hydrolysis of prodrugs **9-16** is FTC (λ<sub>max</sub> = 280 nm, retention time = 2.2 min).  
303 Representative standard curves and prodrug hydrolysis profiles showing analyte resolution  
304 are shown below for conversion of **8** to **16**, and conversion of **16** to FTC. Retention times for  
305 other prodrugs are reported in **Table S1**. Unless otherwise noted, all experiments were  
306 performed in triplicate. Compounds **8** and **16** were utilized to determine inter- and intra-day  
307 accuracy and precision: at the high and middle points of the standard curve these were below  
308 15%; at the low point of the standard curve for both compounds, inter- and intra-day accuracy  
309 and precision were within 20% in accordance with convention

310

311 **Initial rate (human muscle and liver S9) measurements of carbamate cleavage from 9-**  
312 **16 and capecitabine:** Reaction mixtures containing mixed gender human skeletal muscle S9  
313 (10.47 mg/mL, Bioreclamation) or phosphate buffer (0.1 M, pH 7.4) and pooled, mixed

314 gender liver S9 (**9-13**, **15-16** and capecitabine: 10.0 mg/mL; **14**: 5.0 mg/mL) were pre-  
315 incubated at 37 °C for 5 min. Reactions were initiated by the addition of prodrugs **9-16** or  
316 capecitabine (1 mM + 1% DMSO). After incubation at 37 °C, aliquots were taken at time  
317 points measuring initial rate (Muscle S9: CAP, **9-16**: 0.5 min, 1 h, 3 h, 5 h, 24 h, 48 h, 72 h)  
318 (Liver S9: **9**: 0.5 min, 1 h, 2 h, 3 h, 4 h, 5 h, 6 h; **10-11**: 0.5 min, 20 min, 40 min, 60 min, 80  
319 min, 100 min, 120 min; **12-13**: 0.5 min, 10 min, 20 min, 30 min, 40 min, 50 min, 60 min;  
320 CAP and **14-16**: 0.5 min, 5 min, 10 min, 15 min, 20 min, 25 min, 30 min). These aliquots  
321 were quenched in two volumes of ice-cold methanol. The quenched aliquots were then  
322 centrifuged at 16873xg for 5 minutes. The supernatant was diluted 10-fold into phosphate  
323 buffer (0.1 M, pH 7.4) and analyzed by the HPLC method described above monitoring  
324 product depletion at 305 nm.

325 **Half-life (human plasma) measurements of carbamate cleavage from 9-16 and**  
326 **capecitabine:** Reaction mixtures containing pooled mixed gender human plasma  
327 (Bioreclamation) were pre-incubated at 37 °C for 5 min. Reactions were initiated by the  
328 addition of prodrugs **9-16** or capecitabine (1 mM + 1% DMSO). After incubation at 37 °C,  
329 aliquots were taken at the following time points: 0.5 min, 1 h, 3 h, 5 h, 24 h, 48 h, 72 h. These  
330 aliquots were quenched in two volumes of ice-cold methanol. The quenched aliquots were  
331 then centrifuged at 16873xg for 5 minutes. The supernatant was diluted 10-fold into  
332 phosphate buffer (0.1 M, pH 7.4) and analyzed by the HPLC method described above  
333 monitoring product depletion at 305 nm.

334 **Analysis of prodrug stability during SSPN manufacture:** SSPNs were dissolved in DMSO  
335 to yield a prodrug concentration of 100 mM based on the prodrug mass per sample. Samples  
336 were diluted further to 1 mM in DMSO. These stocks were then diluted 10-fold in phosphate  
337 buffer (0.1 M, pH 7.4), giving a final prodrug concentration of 100 µM, prior to HPLC

338 analysis using the following method: 0% to 100% B over 5 minutes at a flow rate of 3 mL  
339  $\text{min}^{-1}$  (solvent A:  $\text{Et}_3\text{NHOAc}$  (50 mM, pH 8), solvent B: acetonitrile). SSPN samples were  
340 compared to two controls: 1) an excipient control comprised of equal masses of excipients  
341 found in SSPNs carried through the same volume and dilution scheme as test samples above,  
342 and 2) a prodrug control comprised of unformulated prodrug at the same concentration as  
343 prodrug found in SSPNs.

344 **Synthesis of semi-solid prodrug nanoparticles via emulsion templated freeze drying**  
345 **with 50 wt% loading of prodrug:** Into separate new 14 mL glass sample vial polymers were  
346 weighed out and dissolved to a final concentration of 13.3 mg/mL, whilst surfactants were  
347 weighed out and dissolved to a final concentration of 10 mg/mL, both in distilled water.  
348 These solutions were left overnight on a rolling mixer to ensure thorough dissolution.  
349 Immediately before synthesis of SSPNs, prodrug was removed from the freezer and weighed  
350 out in to a fresh 14 mL glass vial. Pro drug was dissolved to a final concentration of 50  
351 mg/mL in chloroform and left on a rolling mixer for 10 minutes to ensure thorough  
352 dissolution. Prodrug was not left rolling in solution for any excess time to prevent hydrolysis.  
353 For each SSPN sample, 100  $\mu\text{L}$  of surfactant, 300  $\mu\text{L}$  of polymer, and 100  $\mu\text{L}$  of prodrug was  
354 added to a 4 mL glass sample vial. This was repeated for all 42 combinations of polymer and  
355 surfactant (7x 6) and each prodrug. The final composition yielded SSPNs consisting of 5 mg  
356 prodrug (50 wt%), 1 mg surfactant (10 wt%) and 4 mg polymer (40 wt%). The remainder of  
357 the synthesis process was the same as for SSPNs at 10 wt% loading.

358 **Determination of SSPN candidate formulations:**All samples were dispersed in distilled  
359 water to a final concentration of 1 mg/mL of total prodrug mass. Physical characterisation of  
360 the particles (after dispersion in water) in terms of hydrodynamic diameter and polydispersity  
361 index (PDI) was conducted using DLS Specifically, the following parameters were used:

362 **Particle Type:** Nanoparticles (Refractive Index 1.330, Absorption 0.010)



363 **Dispersant:** Water (Viscosity 0.8872 cP, Refractive Index 1.330)

364 **Temperature:** 25°C

365 **Cell Type:** Polystyrene disposable cuvette

366 **Measurement Angle:** 172° Back Scatter

367 **Number of Measurements:** 3

368 **Number of runs per measurement:** Automatic

369 Candidates were selected based on how easily the dried particle monoliths dispersed in water  
370 (at 1 mg/mL), as well as having Z-average hydrodynamic diameters of less than 700 nm, and  
371 PDI values of less than 0.4.

372

373 **IVIVE Model Equations and Parameters:** The 7-compartment model was generated using  
374 equations from the physB model to simulate organ size, volumes and flow rates  
375 (Supplementary Figure 45).<sup>1</sup> The model generates simulated patients based on  
376 anthropometric measures and allometric scaling. The volume of distribution was simulated  
377 using the Poulin and Theil equation.<sup>2</sup> This method describes the tissue-to-plasma ratio based  
378 on the individual organ volumes generated from the physB equations. The values used in the  
379 model are shown in Supplementary Table 4 and the key equations are described below:

380

381 
$$\frac{\Delta FTC_{oral}}{\Delta t} = Ka * Dose \quad (1)$$

382

383 Equation 1 describes the rate of absorption of FTC following an oral dose where Dose is  
384 equal to the amount of FTC remaining in the oral compartment and Ka is the absorption  
385 constant.

386

387

$$\frac{\Delta Drug_{inj}}{\Delta t} = K_{im} * Dose \quad (2)$$

388

389 Equation 2 describes the rate of release of carbonate carbamate prodrug following an IM dose  
390 where Dose is equal to the amount of carbonate carbamate prodrug remaining in the injection  
391 site and  $K_{im}$  is the release rate.

392

393

$$\frac{\Delta Drug_{inj}}{\Delta t} = Q_{mu} * \left( \frac{IM_{area}}{Muscle_{vol}} \right) * \left( \frac{IM_{drug}}{IM_{area}} \right) \quad (3)$$

394

395 Equation 3 describes the rate of release of carbonate carbamate prodrug, carbamate  
396 intermediate or FTC following an IM dose where  $Q_{mu}$  is equal to the flow rate of blood to  
397 the injection site. Also represented are the area of the injection site ( $IM_{area}$ ), muscle volume  
398 and amount of drug available for release.

399

400

$$\frac{\Delta Drug_{Blood}}{\Delta t} = Cl * Blood_{drug} * R \quad (4)$$

401

402 Equations 4 describes the clearance of carbonate carbamate prodrug, carbamate intermediate  
403 or FTC from the blood accounting for the rate clearance ( $Cl$ ), the blood to plasma ratio ( $R$ )  
404 and the concentration of drug in the blood.

405

406

$$\frac{\Delta Drug_{Li}}{\Delta t} = Q_{hv} * Blood_{drug} - Q_{hv} * Liver_{drug} * \left( \frac{R}{L:P} \right) \quad (5)$$

407

$$\frac{\Delta Drug_{Mu}}{\Delta t} = Q_{mu} * Blood_{drug} - Q_{mu} * Muscle_{drug} * \left( \frac{R}{M:P} \right) \quad (6)$$

408

$$\frac{\Delta Drug_{Ti}}{\Delta t} = Q_{ti} * Blood_{drug} - Q_{ti} * Tissue_{drug} * \left( \frac{R}{T:P} \right) \quad (7)$$

409

410 Equations 5, 6 and 7 describes the transfer of carbonate carbamate prodrug, carbamate  
411 intermediate or FTC to and from liver (Li), muscle (Mu) and peripheral tissues (Ti) where  
412  $Q_{hv}$ ,  $Q_{mu}$  and  $Q_{ti}$  are equal to the flow rate of blood to the liver, muscle and peripheral  
413 tissues respectively. Also represented are the concentration of each drug in the respective  
414 compartments, blood to plasma ratio and the tissue to plasma ratio for liver (L:P), muscle  
415 M:P) and peripheral tissues (T:P).

416

$$417 \quad \frac{\Delta Drug_{Ti}}{\Delta t} = Hyd_1 * PD_1 \quad (8)$$

$$418 \quad \frac{\Delta Drug_{Ti}}{\Delta t} = Hyd_2 * PD_2 \quad (9)$$

419

420 Equations 8 and 9 describe the hydrolysis (Hyd1) of carbonate carbamate prodrug (PD1) to  
421 carbamate intermediate (PD2) and hydrolysis (Hyd2) of carbamate intermediate to FTC. The  
422 rates of hydrolysis are specific to each compartment (plasma, liver or muscle and injection  
423 site) and where determined experimentally.

424

$$425 \quad K_{ic} = \frac{V_{max} * Blood_{drug}}{K_m + Blood_{drug}} \quad (10)$$

$$426 \quad K_{el} = K_{out} * FTC_{TP} \quad (11)$$

427

428 Equation 10 describes the anabolism of FTC to form FTC-TP considering he maximum rate  
429 of uptake ( $V_{max}$ ), the rate of anabolism ( $K_m$ ) and the concentration of FTC in the blood.

430 Equation 11 shows the rate of elimination of intracellular FTC-TP which is determined by the  
431 elimination rate constant ( $K_{out}$ ).

432

433 **Simulation design:** A virtual cohort of 50 patients was generated, and a simulated once-daily  
434 dose of FTC (400 mg) was validated against clinical data at steady state. The validated model

435 was then used for LA simulations, IM dose of 2g SSPN over 28 days. Patient age (minimum  
436 of 18 years and maximum of 60 years), weight (minimum of 40 kg and maximum of 100 kg),  
437 height (minimum of 1.5 m and maximum of 2.1 m), and body mass index (minimum of 18  
438 and maximum of 30) were generated from random normally distributed values.

439

440 **Details of ad hoc IVIVE modelling:** In order to explore the variability in patient data the  
441 model was validated against 3 clinical studies (all at steady state receiving a once daily dose  
442 of 200mg FTC).<sup>3-5</sup> In order to increase the predictive quality of the simulated data, key model  
443 parameters were fit to better represent the data (Supplementary Table 8). The simulated data  
444 showed acceptable deviation from the observed clinical data. The  $C_{max}$ ,  $C_{min}$  and AUC varied  
445 by +4%, -53% and +52% respectively (Supplementary Table 9). Simulated FTC plasma  
446 concentrations fell below the concentration inhibiting 90% of viral replication ( $IC_{90}$ , 50  
447 ng/mL) at 13 and 22 days for **4** and **8**, respectively. Simulated intracellular FTC-TP  
448 (Supplementary Tables 10 & 11)  $C_{min}$  at day 28 maintained simulated intracellular  
449 concentrations above the intracellular  $IC_{50}$ , 332 ( $\pm$  132.3) fmol/ $10^6$  cells and 444 ( $\pm$  197.1)  
450 fmol/ $10^6$  cells. The simulated data indicate that even when the model is fit to a range of  
451 clinical data, SSPNs of prodrugs **4** and **8** have the potential to sustain concentrations of FTC  
452 above the intracellular  $IC_{50}$  for 28 days following a single 2 g IM injection.

453

454

455

456

457

458

459

460

461

### Supplementary References

462

1. Bosgra S, van Eijkeren J, Bos P, Zeilmaker M, Slob W. An improved model to predict physiologically based model parameters and their inter-individual variability from anthropometry. *Crit. Rev. Toxicol.*, 2012, **42**, 751–767

463

464

465

2. Poulin P, Theil FP. Prediction of pharmacokinetics prior to in vivo studies. 1. Mechanism-based prediction of volume of distribution. *J. Pharm. Sci.*, 2002. **91**,129 – 156.

466

467

468

469

470

471

3. Molina J-M, Peytavin G, Perusat S, Lascoux-Combes C, Sereni D, Rozenbaum W, Chene G. Pharmacokinetics of emtricitabine, didanosine and efavirenz administered once-daily for the treatment of HIV-infected adults (pharmacokinetic sub-study of the ANRS 091 trial). *HIV Med.*, 2004, **5**, 99-104.

472

473

474

475

4. Wang LH, Begley J, St Claire RL 3rd, Harris J, Wakeford C, Rousseau FS. Pharmacokinetic and pharmacodynamic characteristics of emtricitabine support its once daily dosing for the treatment of HIV infection. *AIDS Res Hum Retroviruses*, 2004, 20, 1173-82.

476

477

478

5. [https://liverpool-hiv-hep.s3.amazonaws.com/prescribing\\_resources/pdfs/000/000/063/original/HIV\\_FactSheet\\_FTC\\_2016\\_Mar.pdf?1520612387](https://liverpool-hiv-hep.s3.amazonaws.com/prescribing_resources/pdfs/000/000/063/original/HIV_FactSheet_FTC_2016_Mar.pdf?1520612387) accessed on 26<sup>th</sup> November 2018

479